

Supporting information

Harnessing Solvation-Guided Engineering to Enhance Deep Eutectic Solvent Resistance and Thermostability in Enzymes

Yijie Sheng¹, Haiyang Cui², Xinyue Wang¹, Minghui Wang¹, Ping Song¹, He Huang¹, Xiujuan Li^{1}*

¹College of Food Science and Pharmaceutical Engineering, Nanjing Normal University, Nanjing 210097, China.

²College of Life Sciences, Nanjing Normal University, Nanjing 210046, China.

*Corresponding author: Xiujuan Li, Email: lixiujuan@njnu.edu.cn

Contents

Experimental.....	6
Preparation of deep eutectic solvent.....	6
Generation of BSLA variants by mutagenesis.....	6
Protein expression and DES resistance measurement	6
The p-Nitrophenyl butyrate assay for measuring BSLA activity	7
Determination of thermostability profiles	7
In silico generation of variants and stability analysis.....	8
Molecular dynamics simulations	8
Section S1. Analysis of the overall structure and solvation phenomena of BSLA WT under different concentrations of DES	10
Section S2. Analysis of interaction energy of BSLA in DESs	10
Section S3. Analysis of the conformational change in BSLA active site.....	11
Table S1. Primers used for solvation-guided engineering of BSLA.	12
Table S2. Summary of calculated observables during MD simulation.	15
Table S3. The solvation score of BSLA for each of surface amino acids in 30% (v/v) ChCl:Acetamide (1:2).....	16
Table S4. The solvation score of BSLA for each of surface amino acids in 30% (v/v) TBPB:EG (1:2).	17
Table S5. The solvation score of BSLA for each of surface amino acids in 95% (v/v) ChCl:EG (1:2).....	18
Table S6. Stability analysis of the BSLA variants.	19
Figure S1. The 100 ns root mean square deviation (RMSD) of BSLA backbone with respect to the initial structure as a function of time.....	20
Figure S2. Time averaged radius of gyration of BSLA determined from the last 40 ns of MD simulations.	21
Figure S3. Time averaged Internal Hydrogen bond of BSLA determined from the last 40 ns of MD simulations.....	22
Figure S4. RMSF of BSLA residues.	23

Figure S5. The time-averaged total solvent accessible surface area (SASA), hydrophobic SASA, and hydrophilic SASA of BSLA WT.....	24
Figure S6. DES layer around BSLA.....	25
Figure S7. H-bond acceptor layer around BSLA.....	26
Figure S8. H-bond donor layer around BSLA.....	27
Figure S9. Spatial distribution of DES and water molecules at the enzyme surface in 30% (v/v) TBPB:EG, and 95% (v/v) ChCl:EG.....	28
Figure S10. The RDFs were calculated in ChCl: acetamide and TBPB: EG systems.	29
Figure S11. The water number in substrate binding cleft (SBC) of BSLA.....	30
Figure S12. The number of DES molecule in substrate binding cleft (SBC) of BSLA.	31
Figure S13. The number of DES donor in substrate binding cleft (SBC) of BSLA.....	32
Figure S14. Time averaged energy of protein with water molecules.	33
Figure S15. Time averaged energy of protein with DES molecules.	34
Figure S16. Time averaged energy of protein with DES acceptor.	35
Figure S17. Time averaged energy of protein with DES donor.	36
Figure S18. The interaction of residue (G175, G176, and R147) of BSLA with DES molecules (choline ⁺ , acetamide, tetrabutylphosphonium ⁺ , and ethylene glycol).....	37
Figure S19. The number of water molecules around each amino acid type at the surface of BSLA WT in 100% water simulation system.	38
Figure S20. The number of DES molecules around each amino acid type at the surface of BSLA WT in 30% ChCl:Acetamide (1:2) simulation system.	39
Figure S21. The number of water molecules around each amino acid type at the surface of BSLA WT in 30% ChCl:Acetamide (1:2) simulation system.	40
Figure S22. The number of DES molecules around each amino acid type at the surface of BSLA WT in 100% (v/v) ChCl:Acetamide (1:2) simulation system.....	41
Figure S23. The number of water molecules around each amino acid type at the surface of BSLA WT in 30% (v/v) TBPB:EG (1:2) simulation system.	42
Figure S24. The number of DES molecules around each amino acid type at the surface of BSLA WT in 30% (v/v) TBPB:EG (1:2) simulation system.	43

Figure S25. The number of DES molecules around each amino acid type at the surface of BSLA WT in 100% (v/v) TBPB:EG (1:2) simulation system.	44
Figure S26. The number of DES molecules around each amino acid type at the surface of BSLA WT in 95% (v/v) ChCl:EG (1:2) simulation system.	45
Figure S27. The number of water molecules around each amino acid type at the surface of BSLA WT in 95% (v/v) ChCl:EG (1:2) simulation system.	46
Figure S28. The number of DES molecules around each amino acid type at the surface of BSLA WT in 100% (v/v) ChCl:EG (1:2) simulation system.	47
Figure S29. The residual activity of BSLA variants at 50°C as a function of time.	48
Figure S30. Root-mean-square deviation (RMSD) of the BSLA backbone with respect to the initial structure as a function of time in 30% (v/v) ChCl:Acetamide (1:2), 30% (v/v) TBPB:EG (1:2) and 95% (v/v) ChCl:EG (1:2).	49
Figure S31. The time-averaged radius of gyration (R _g) of BSLA variants in 30% (v/v) ChCl:Acetamide (1:2), 30% (v/v) TBPB:EG (1:2) and 95% (v/v) ChCl:EG (1:2).	50
Figure S32. The time-averaged SASA of BSLA variants.	51
Figure S33. RMSF of BSLA variants in 30% (v/v) ChCl:Acetamide (1:2), 30% (v/v) TBPB:EG (1:2) and 95% (v/v) ChCl:EG (1:2) averaged over the last 40 ns of MD trajectories.	52
Figure S34. Local RMSF of BSLA variants in (a) 30% (v/v) TBPB:EG (1:2) and (b) 95% (v/v) ChCl:EG (1:2) averaged over the last 40 ns of MD trajectories.	53
Figure S35. DES layer around BSLA variants in 30% (v/v) ChCl:Acetamide (1:2), 30% (v/v) TBPB:EG (1:2) and 95% (v/v) ChCl:EG (1:2) averaged over the last 40 ns of MD trajectories.	54
Figure S36. Hydration shell around BSLA variants in 30% (v/v) ChCl:Acetamide (1:2), 30% (v/v) TBPB:EG (1:2) and 95% (v/v) ChCl:EG (1:2) averaged over the last 40 ns of MD trajectories.	55
Figure S37. The number of DES molecule in substrate binding cleft (SBC) of BSLA variants in 30% (v/v) ChCl:Acetamide (1:2), 30% (v/v) TBPB:EG (1:2) and 95% (v/v) ChCl:EG (1:2) averaged over the last 40 ns of MD simulations.	56

Figure S38. The number of increased water molecules in substrate binding cleft (SBC) of BSLA variants in 30% (v/v) ChCl:Acetamide (1:2), 30% (v/v) TBPB:EG (1:2) and 95% (v/v) ChCl:EG (1:2) averaged over the last 40 ns of MD simulations.....	57
Figure S39. Distance of active site of BSLA variants.	58

Experimental

Preparation of deep eutectic solvent

Three DES (ChCl:Acetamide, TBPB:EG, ChCl:EG) were prepared by the heating method as previously reported.¹ The components were weighed in molar ratio and placed in a 50 mL conical flask. The mixture was heated in water bath up to 90 °C while being stirred until clear liquid was formed. The DES was formed in a clear liquid manner after heating, and was kept at room temperature for 24 hours before application. The preheated DES, heated to approximately 80°C, was utilized to generate DES solutions across a concentration range of 0– 100% (v/v) through gradual dilution with TEA buffer (pH 7.4, 50 mM).

Generation of BSLA variants by mutagenesis

The previously constructed plasmid pET22b (+)-bsla wild type was used as a template to construct the single substitutions by the site-directed mutagenesis (SDM) method and recombinants were constructed by stepwise SDM.² The primers are shown in **Table S1**. The variants were verified by sequencing.

Protein expression and DES resistance measurement

Chemically competent *Escherichia coli* DH5a and *E. coli* BL21-Gold (DE3) (Tsingke Biological Technology, China) were used as hosts for plasmids amplification and protein expression, respectively. The detailed description of the BSLA expression and the activity assay with *p*-Nitrophenyl butyrate (*p*NPB) in 96-well MTP was reported in our previous studies.³ DES resistance of BSLA (wild type or variant) was evaluated as activity in the presence of DES divided by activity in the absence of DES.

$$\text{Residual activity} = \frac{\text{slope}_{WT/Variant \text{ in DES cosolvent}} - \text{slope}_{EV \text{ in DES cosolvent}}}{\text{slope}_{WT/Variant \text{ in buffer}} - \text{slope}_{EV \text{ in buffer}}}$$

$$\text{Resistance fold} = \frac{\text{Residual activity}_{\text{variant}}}{\text{Residual activity}_{\text{BSLA}}}$$

EV: empty vector. The concentration of DES (30% (v/v) ChCl:Acetamide, 30% (v/v) TBPB:EG, and 95% (v/v) ChCl:EG) resulting in a residual BSLA activity of 30-40% were chosen for the experiment to keep an effective screening window as suggested in previous studies. ⁴ The beneficial substitution was defined as a substitution that increases BSLA resistance fold to the respective DES.

The p-Nitrophenyl butyrate assay for measuring BSLA activity

The residual activity of BSLA variant was measured at room temperature (25 °C) with *p*-Nitrophenyl butyrate (*p*NPB) as substrate at different concentrations of the three DESs. Microplate incubation was performed in LB_{Amp} medium (150 µL per well) at 37 °C, 70% humidity, 900 rpm overnight, and 96-well expression cultivation was performed in modified autoinduction_{Amp} medium at 16 h, 37 °C, 70% humidity, and 900 rpm. Cells were harvested by centrifugation at 5000 g for 30 min, followed by resuspended in buffer (pH 7.5, 25 mM Tris-Cl, 150 mM NaCl, 10 mM imidazole, and 0.5 mg/mL lysozyme) for lysis (1h, 37 °C). After centrifugation (5000 g for 20 min), the supernatant (5 µL) was added to 95 µL of assay buffer per well. The liberation of *p*-nitrophenyl cresol was documented by measuring A_{410nm} within 8 min at room temperature with a microtiter plate reader (Biotek Synergy HI, USA) as in our previous study. ³

Determination of thermostability profiles

Residual activity was measured after incubation for 60 min of BSLA WT and variants at different temperatures from 30 to 100 °C using *p*NPB as substrate. The residual activity at room temperature (25 °C) was defined as 100%. Half-life(*t*_{1/2}) was defined as the time required for enzyme variants to reach half of their initial value of residual

activity. To measure the $t_{1/2}$ value, the activity was monitored by incubating the crude BSLA protein at 50 °C.

In silico generation of variants and stability analysis

The crystal structure of BSLA (PDB ID: 1i6w, ⁵ Chain A, resolution 1.5 Å) was used as a model for the generation of variants containing single and multiple substitutions by the FoldX approach using the YASARA Plugin in YASARA structure version 17.4.17. The parameters of FoldX were established as 0.05 M for ionic strength, 298 K for temperature, and pH 7. ⁶ Meanwhile, $\Delta\Delta G_{\text{fold}}$ ($\Delta\Delta G_{\text{fold}} = \Delta G_{\text{fold, sub}} - \Delta G_{\text{fold, wt}}$) were calculated for evaluating the thermodynamic stability of the variants as previous reported. ⁶

Molecular dynamics simulations

MD simulations of BSLA WT and variants were performed using the GROMACS 2022 software package and GROMOS96(54a7) force field in various DESs. ⁷ GROMOS96(54a7) force field was applied for studying the DES-enzyme interaction previously.⁸ The crystal structure of BSLA chain with PDB ID 1i6w was obtained from Protein Data Bank (3-181 amino acids). ⁵ The DES models were obtained from ATB (<https://atb.uq.edu.au>) ⁹ with the optimized parameters set matching GROMOS96(54a7) force field. Protein protonation was performed using the gmx self-contained tool gmx pdb2gmx, and the protein molecules were placed in a cubic box (12 Å from the edge of the box). Depending on the DES concentration, a corresponding number of ~140 choline cation ions, ~140 chloride anion ions and ~280 acetamide molecules in 30% (v/v) ChCl:Acetamide (1:2) system, ~468 choline cation ions, ~468 chloride anion ions and ~936 acetamide molecules in 100% (v/v) ChCl:Acetamide (1:2) system, ~56 tetrabutylphosphonium cation ions, ~56 bromine anion ions and ~112 ethylene glycol molecules in 30% (v/v) TBPB:EG (1:2) system, ~187 tetrabutylphosphonium cation

ions, ~187 bromine anion ions and ~374 ethylene glycol molecules in 100% (v/v) TBPB:EG (1:2) system, ~424 choline cation ions, ~424 chloride anion ions and ~848 ethylene glycols molecules in 95% (v/v) ChCl:EG (1:2) system, and ~446 choline cation ions, ~446 chloride anion ions and ~892 ethylene glycols molecules in 100% (v/v) ChCl:EG (1:2) system were added to the box. Afterwards, the rest of the system (30% (v/v) ChCl:Acetamide (1:2), 30% (v/v) TBPB:EG (1:2), 95% (v/v) ChCl:EG (1:2)) were filled with SPCE water model.¹⁰ The charge of the system was neutralized with Na⁺ and Cl⁻, and the net charge was zero in all setup systems.

Energy minimization was first performed using the steepest descent method to avoid the most unfavorable interactions.¹¹ As in our previous studies,^{3,12} NVT tethering was performed at temperatures close to 298 K for 100 ps, followed by equilibration in NPT tethering for 100 ps with positional constraints on the protein structure. We performed three independent MD simulations for each BSLA-DES system with different atomic onset velocities to avoid artifacts (100 ns at 298 K with a time step of 1 bar at 1 ps). Coordinates, energies, and velocities were collected every 0.5 ns for the subsequent analysis with the GROMACS simulation package tool. The results were visualized and analyzed using PYMOL 2.5.2,¹³ VMD 1.9.4,¹⁴ and GROMACS tools.¹⁵ We performed overall structural analysis of the protein (including root mean square deviation (RMSD), radius of gyration (R_g), root mean square fluctuation (RMSF), Hydrogen Bond, solvent accessible surface area (SASA), and the distance transformation of the active site), solvation phenomenon analysis (including the overall hydration shell, DES layer, spatial distribution function (SDF), radial distribution function (RDF), and the number of water and DES molecules in active site), and interaction energy analysis of the protein with solvent molecules as a comprehensive assessment of the impact for DES cosolvent on BSLA.

Section S1. Analysis of the overall structure and solvation phenomena of BSLA WT under different concentrations of DES

The RMSD of 100ns (**Figure S1**) indicated that all simulated systems reached equilibrium in the last 40ns without large fluctuations. The time averaged radius of gyration (Rg) (**Figure S2**) values of BSLA WT at different concentrations of DES were slightly reduced to those of 100% (v/v) water system. The number of internal hydrogen bonds (**Figure S3**) showed a different degree of increase. Meanwhile, the RMSF values for the individual residue of BSLA WT were shown in **Figure S4**, varying between 0.5 Å and 4.0 Å, and the value in DES systems was less than 100% (v/v) water system. The time-averaged total solvent accessible surface area (SASA), hydrophobic SASA, and hydrophilic SASA (**Figure S5**) of BSLA WT showed no remarkable changed trend. The DES layer (**Figure S6**), H-bond acceptor layer (**Figure S7**), and H-bond donor layer (**Figure S8**) around BSLA displayed the same tendency. The Spatial distribution (**Figure S9**) of DES and water molecules at BSLA surface revealed the stripping effect of DES on water molecules. The number of water molecule (**Figure S11**), DES molecule (**Figure S12**), and DES donor (**Figure S13**) in substrate binding cleft (SBC) demonstrated that DES molecule stripped water molecule from SBC.

Section S2. Analysis of interaction energy of BSLA in DESs

Furthermore, the non-bond binding free energies ($\Delta G_{\text{non-bond}}$), electrostatic energy (ΔE_{elec}), and van der Waals energy (ΔE_{vdw}) were calculated to examine the strength of water/DES molecule binds to BSLA. Time averaged energy of protein with water molecules (**Figure S14**), protein with DES molecules (**Figure S15**), protein with DES acceptor (**Figure S16**), and protein with DES donor (**Figure S17**) were used to visualize the energy landscape between protein and DES molecules and water molecules. We discovered that $\Delta G_{\text{non-bond}}$ between DES molecules and protein ranged from 1.8- to 4.5-folds of that between water molecules and protein in 30% (v/v) ChCl:Acetamide, 30% (v/v) TBPB:EG, and 95% (v/v) ChCl:EG. Interestingly, in the systems of 30% (v/v) ChCl:Acetamide and 100% (v/v) ChCl:EG, the DES acceptor occupied the major part of the DES-protein binding energy, whereas in the systems of 30% (v/v) TBPB:EG, 100% (v/v) TBPB:EG, 100% (v/v) ChCl:Acetamide, and 30% (v/v) ChCl:EG systems, the DES donor dominated the DES-protein binding energy. It indicated that different

systems as well as different concentrations of DES, would affect the interaction binding energies with protein. The interaction of residue of BSLA with DES molecules (**Figure S18**) indicated the formation of hydrogen bonding interaction forces between DES molecules and protein.

Section S3. Analysis of the conformational change in BSLA active site

As shown in **Figure S39**, we discovered that the distance among catalytic triad in the active site of all BSLA recombinant in ChCl:Acetamide was increased compared to WT, but not consistent conformational changes were shown in the other two DES systems.

Table S1. Primers used for solvation-guided engineering of BSLA.

Name	5 --> 3 sequence
H3L Forward Primer	GGATATCGCTGAACTGAATCCAGTCGTTAT
H3L Reverse Primer	ATAACGACTGGATTCAGTTCAGCGATATCC
H3V Forward Primer	GGATATCGCTGAAGTTAATCCAGTCGTTAT
H3V Reverse Primer	ATAACGACTGGATTA <u>AACT</u> TTCAGCGATATCC
R33L Forward Primer	CAGGGCTGGTCGCTGGACAAGCTGTAT
R33L Reverse Primer	ATACAGCTTGTCCAGCGACCAGCCCTG
R33V Forward Primer	CAGGGCTGGTCGTTGACAAGCTGTAT
R33V Reverse Primer	ATACAGCTTGTCA <u>ACCG</u> ACCAGCCCTG
D34H Forward Primer	GGCTGGTCGCGGCATAAAGCTGTATGCA
D34H Reverse Primer	TGCATACAGCTTATGCCGCGACCAGCC
D34Y Forward Primer	GGCTGGTCGCGGTATAAAGCTGTATGCA
D34Y Reverse Primer	TGCATACAGCTTAT <u>ACCG</u> CGACCAGCC
D40H Forward Primer	AGCTGTATGCAGTTC <u>ACT</u> TTTTGGGACAAGAC
D40H Reverse Primer	GTCTTGTCCCAAAGTGAAGTGCATACAGCT
D40Y Forward Primer	AGCTGTATGCAGTTTATTTTTGGGACAAGAC
D40Y Reverse Primer	GTCTTGTCCCAA <u>AAATA</u> AACTGCATACAGCT
D43H Forward Primer	AGTTGATTTTTGGCATAAAGACAGGCACAA
D43H Reverse Primer	TTGTGCCTGTCTTATGCCAAAATCAACT
D43Y Forward Primer	AGTTGATTTTTGGTATAAAGACAGGCACAA
D43Y Reverse Primer	TTGTGCCTGTCTTAT <u>ACCA</u> AAAATCAACT
R57L Forward Primer	ACCGGTATTATCACTGTTTGTGCAAAGG
R57L Reverse Primer	CCTTTTGCACAAACAGTGATAATACCGGT
R57V Forward Primer	ACCGGTATTATCAGTTTTTGTGCAAAGG
R57V Reverse Primer	CCTTTTGCACAAA <u>ACT</u> GATAATACCGGT
D64H Forward Primer	GCAAAGGTTTTACACGAAACGGGTGCG
D64H Reverse Primer	CGCACCCGTTTCGTGTAACCTTTTGC
D64Y Forward Primer	GCAAAGGTTTTATACGAAACGGGTGCG
D64Y Reverse Primer	CGCACCCGTTTCGTATAAACCTTTTGC
E65H Forward Primer	AAGGTTTTAGATCATACGGGTGCGAAAAAAG
E65H Reverse Primer	CTTTTTTCGCACCCGTATGATCTAAAACCTT
E65Y Forward Primer	AAGGTTTTAGATTATACGGGTGCGAAAAAAG

E65Y Reverse Primer	CTTTTTTCGCACCCGTATAATCTAAAACCTT
D91H Forward Primer	CTACATAAAAAATCTGCATGGCGGAAATAAAGTTG
D91H Reverse Primer	CAACTTTATTTCCGCCATGCAGATTTTTTATGTAG
D91Y Forward Primer	CTACATAAAAAATCTGTATGGCGGAAATAAAGTTG
D91Y Reverse Primer	CAACTTTATTTCCGCCATACAGATTTTTTATGTAG
R107L Forward Primer	GGCGGCGCGAACCTGTTGACGACAGGC
R107L Reverse Primer	GCCTGTTCGTC AACAGGTTTCGCGCCGCC
R107V Forward Primer	GGCGGCGCGAACGTTTTGACGACAGGC
R107V Reverse Primer	GCCTGTTCGTC AAAACGTTTCGCGCCGCC
D118H Forward Primer	CGCTTCCGGGAACACACCCAAATCAAAGAT
D118H Reverse Primer	ATCTTTTGATTTGGGTGTGTTCCCGGAAGCG
D118Y Forward Primer	CGCTTCCGGGAACATATCCAAATCAAAGAT
D118Y Reverse Primer	ATCTTTTGATTTGGATATGTTCCCGGAAGCG
D133H Forward Primer	TTTACAGCAGTGCCACATGATTGTCATGAA
D133H Reverse Primer	TTCATGACAATCATGTGGGCACTGCTGTAAA
D133Y Forward Primer	TTTACAGCAGTGCCATATGATTGTCATGAA
D133Y Reverse Primer	TTCATGACAATCATATAGGCACTGCTGTAAA
R142L Forward Primer	CATGAATTA CTTATCACTGTTAGATGGTGCTAGAA
R142L Reverse Primer	TTCTAGCACCATCTAACAGTGATAAGTAATTCATG
R142V Forward Primer	CATGAATTA CTTATCAGTTTTAGATGGTGCTAGAA
R142V Reverse Primer	TTCTAGCACCATCTAAA ACTGATAAGTAATTCATG
D144H Forward Primer	TACTTATCAAGATTACACGGTGCTAGAAACGTTCA
D144H Reverse Primer	TGAACGTTTCTAGCACCGTGTAATCTTGATAAGTA
D144Y Forward Primer	TACTTATCAAGATTATATGGTGCTAGAAACGTTCA
D144Y Reverse Primer	TGAACGTTTCTAGCACCATATAATCTTGATAAGTA
R147L Forward Primer	GATTAGATGGTGCTCTGAACGTTCAAATCCA
R147L Reverse Primer	TGGATTTGAACGTT CAGAGCACCATCTAATC
R147V Forward Primer	GATTAGATGGTGCTGTTAACGTTCAAATCCA
R147V Reverse Primer	TGGATTTGAACGTT AACAGCACCATCTAATC
H152L Forward Primer	AACGTTCAAATCCTGGGCGTTGGACAC
H152L Reverse Primer	GTGTCCAACGCC CAGGATTTGAACGTT
H152V Forward Primer	AACGTTCAAATCGTTGGGCGTTGGACAC
H152V Reverse Primer	GTGTCCAACGCC AACGATTTGAACGTT

H156L Forward Primer	CATGGCGTTGG <u>ACTGAT</u> CGGCCTTCTG
H156L Reverse Primer	CAGAAGGCCGAT <u>CAGT</u> CCAACGCCATG
H156V Forward Primer	CATGGCGTTGGAG <u>TTAT</u> CGGCCTTCTG
H156V Reverse Primer	CAGAAGGCCGATA <u>ACT</u> CCAACGCCATG
E171H Forward Primer	AGCCTGATTA <u>AAACAC</u> GGGCTGAACGGC
E171H Reverse Primer	GCCGTT <u>CAGCCC</u> GTGTTTAATCAGGCT
E171Y Forward Primer	AGCCTGATTA <u>AAATAT</u> GGGCTGAACGGC
E171Y Reverse Primer	GCCGTT <u>CAGCCC</u> ATATTTAATCAGGCT

Table S2. Summary of calculated observables during MD simulation.

Descriptor	Location	Observables	Results	Determinant
Geometrical property	Overall protein	100 ns RMSD	Figure S1	no
		Time-averaged RMSD	Figure 2a	no
		Time-averaged R_g	Figure S2	no
		Internal H-bond	Figure S3	no
		RMSF	Figure S4	no
		Total SASA	Figure S5	no
		Hydrophobic SASA	Figure S5	no
		Hydrophilic SASA	Figure S5	no
	Active site	Distance of Ser77-OG \cdots Asp133-OD1	Figure 2b	no
		Distance of Ser77-OG \cdots His156-ND1	Figure 2b	no
Distance of Asp133-OD1 \cdots His156-ND1		Figure 2b	no	
Solvation phenomenon	Overall protein	Hydration shell	Figure 2c	yes
		DES layer	Figure S6	yes
		H-bond acceptor layer	Figure S7	yes
		H-bond donor layer	Figure S8	yes
		SDF	Figure S9	yes
		RDF	Figure S10	no
	Active site	Number of water molecule	Figure S11	yes
		Number of DES molecule	Figure S12	yes
		Number of DES acceptor	Figure 2d	yes
		Number of DES donor	Figure S13	yes
Interaction energy	Overall protein	ΔE_{elec} (BSLA-water)	Figure S14	no
		ΔE_{vdW} (BSLA-water)	Figure S14	no
		$\Delta G_{\text{non-bond}}$ (BSLA-water)	Figure S14	no
		ΔE_{elec} (BSLA-DES)	Figure S15	no
		ΔE_{vdW} (BSLA-DES)	Figure S15	no
		$\Delta G_{\text{non-bond}}$ (BSLA-DES)	Figure S15	no
		ΔE_{elec} (BSLA-DES acceptor)	Figure S16	no
		ΔE_{vdW} (BSLA-DES acceptor)	Figure S16	no
		$\Delta G_{\text{non-bond}}$ (BSLA-DES acceptor)	Figure S16	no
		ΔE_{elec} (BSLA-DES donor)	Figure S17	no
		ΔE_{vdW} (BSLA-DES donor)	Figure S17	no
$\Delta G_{\text{non-bond}}$ (BSLA-DES donor)	Figure S17	no		
In total		33		

Table S3. The solvation score of BSLA for each of surface amino acids in 30% (v/v) ChCl:Acetamide (1:2).

30% (v/v) ChCl:Acetamide (1:2)	score
E	-31.4
D	-15.4
W	-11.1
N	-2.9
P	-1.1
A	-1.0
V	-0.9
G	-0.3
L	-0.2
T	0.0
M	1.4
F	1.5
S	2.5
I	2.8
Q	3.0
R	4.3
K	4.6
H	7.0
Y	7.5

Table S4. The solvation score of BSLA for each of surface amino acids in 30% (v/v) TBPB:EG (1:2).

30% (v/v) TBPB: EG (1:2)	score
E	-20.4
D	-12.2
W	-6.2
K	-5.9
N	-3.5
A	-2.5
P	-2.5
Q	-2.2
R	-1.8
L	-1.6
G	-0.8
S	-0.5
V	-0.2
F	-0.1
T	-0.1
M	2.0
I	2.2
Y	3.2
H	4.7

Table S5. The solvation score of BSLA for each of surface amino acids in 95% (v/v) ChCl:EG (1:2).

95% (v/v) ChCl: EG (1:2)	score
R	-19.0
H	-17.9
W	-16.4
N	-15.5
Q	-15.3
D	-15.3
K	-13.9
Y	-12.7
F	-12.3
E	-10.4
S	-9.0
T	-7.8
M	-6.7
P	-5.3
A	-5.0
G	-4.9
I	-4.5
V	-4.3
L	-4.1

Table S6. Stability analysis of the BSLA variants.

BSLA variant	Sum $\Delta\Delta G_{\text{fold}}$ of substitutions (kcal/mol)	Overall $\Delta\Delta G_{\text{fold}}$ of recombinant (kcal/mol)
D64H/R142L	-0.78	-0.69
R107L/E171Y	-0.68	-1.42
D64H/R107L/E171Y	-1.31	-1.92
D64H/R142L/E171Y	-1.31	-1.19

The command (Mutate residue) was applied to calculate the $\Delta\Delta G_{\text{fold}}$ of every single substitution. $\text{Sum } \Delta\Delta G_{\text{fold}} = \Delta\Delta G_{\text{fold, sub1}} + \Delta\Delta G_{\text{fold, sub2}} + \Delta\Delta G_{\text{fold, subX}}$. The command (Mutate multiple residues) was applied to calculate the overall $\Delta\Delta G_{\text{fold}}$ of recombinants. Due to the accuracy of the FoldX method in the prediction of relative folding free energies is reported to be 0.46 kcal/mol, and we defined that the synergistic effect occurs when $(\text{Sum of } \Delta\Delta G_{\text{fold}} - \text{Overall } \Delta\Delta G_{\text{fold}}) > 0.46$ kcal/mol. The $\Delta\Delta G_{\text{fold}}$ calculations were performed three times and averaged for each variant overall $\Delta\Delta G_{\text{fold}}$ of recombinants.

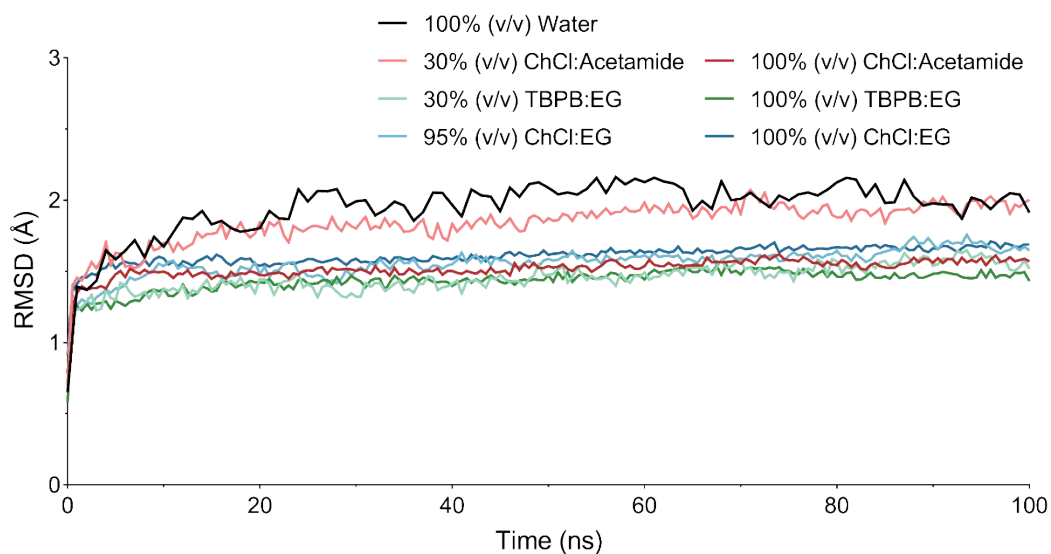


Figure S1. The 100 ns root mean square deviation (RMSD) of BSLA backbone with respect to the initial structure as a function of time. All DES systems 30% (v/v) ChCl:Acetamide, 100% (v/v) ChCl:Acetamide, 30% (v/v) TBPB:EG, 100% (v/v) TBPB:EG, 95% (v/v) ChCl:EG and 100% (v/v) ChCl:EG have a molar ratio of 1:2. The data averaged from three independent runs.

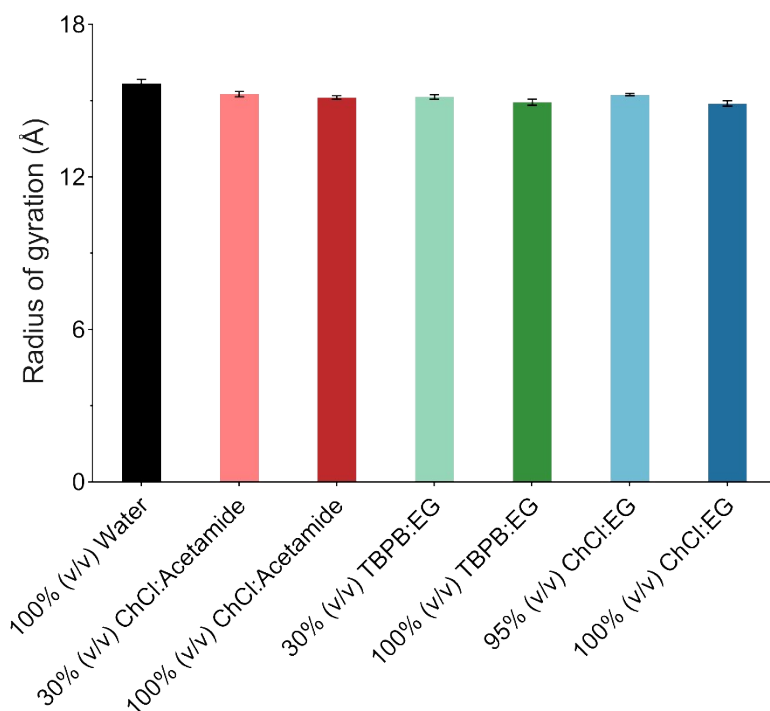


Figure S2. Time averaged radius of gyration of BSLA determined from the last 40 ns of MD simulations. All DES systems 30% (v/v) ChCl:Acetamide, 100% (v/v) ChCl:Acetamide, 30% (v/v) TBPB:EG, 100% (v/v) TBPB:EG, 95% (v/v) ChCl:EG and 100% (v/v) ChCl:EG have a molar ratio of 1:2. Error bars correspond to the standard deviation of three independent MD runs.

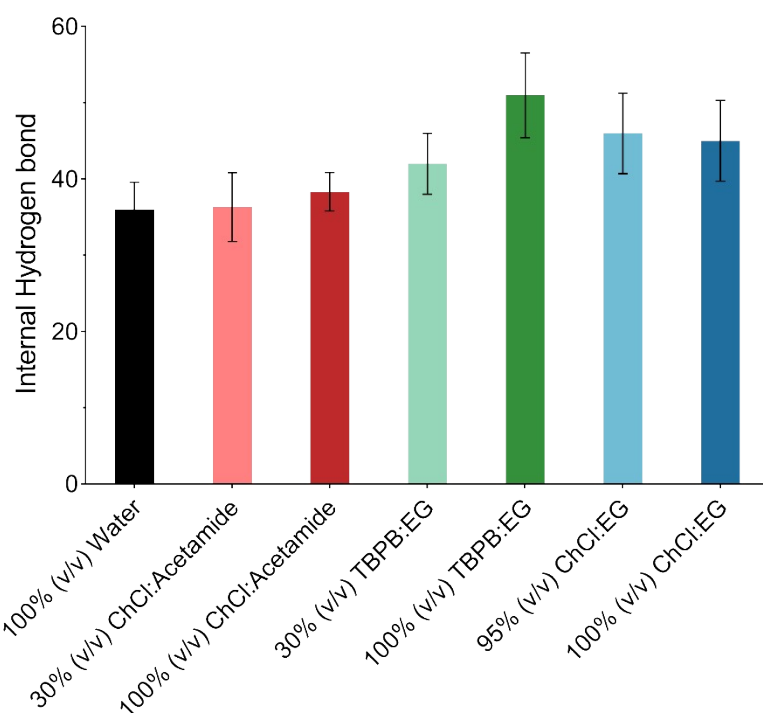


Figure S3. Time averaged Internal Hydrogen bond of BSLA determined from the last 40 ns of MD simulations. All DES systems 30% (v/v) ChCl:Acetamide, 100% (v/v) ChCl:Acetamide, 30% (v/v) TBPB:EG, 100% (v/v) TBPB:EG, 95% (v/v) ChCl:EG and 100% (v/v) ChCl:EG have a molar ratio of 1:2. Error bars correspond to the standard deviation of three independent MD runs.

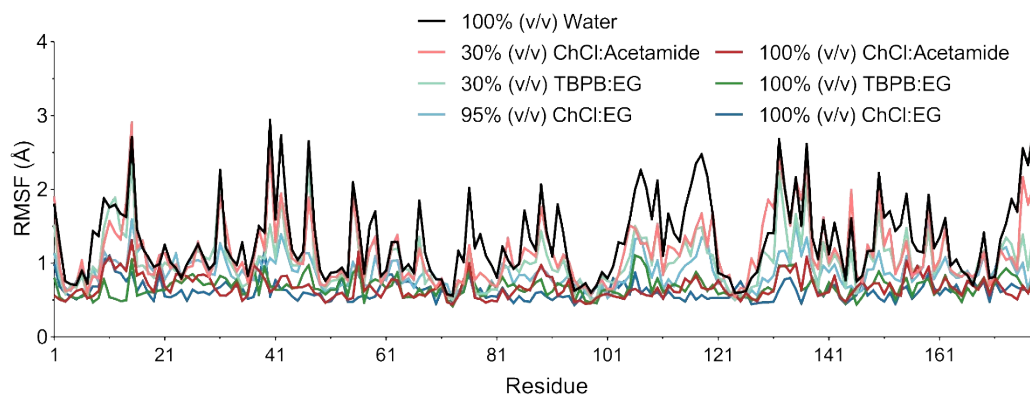


Figure S4. RMSF of BSLA residues. All DES systems 30% (v/v) ChCl:Acetamide, 100% (v/v) ChCl:Acetamide, 30% (v/v) TBPB:EG, 100% (v/v) TBPB:EG, 95% (v/v) ChCl:EG and 100% (v/v) ChCl:EG have a molar ratio of 1:2. The data averaged from three independent runs.

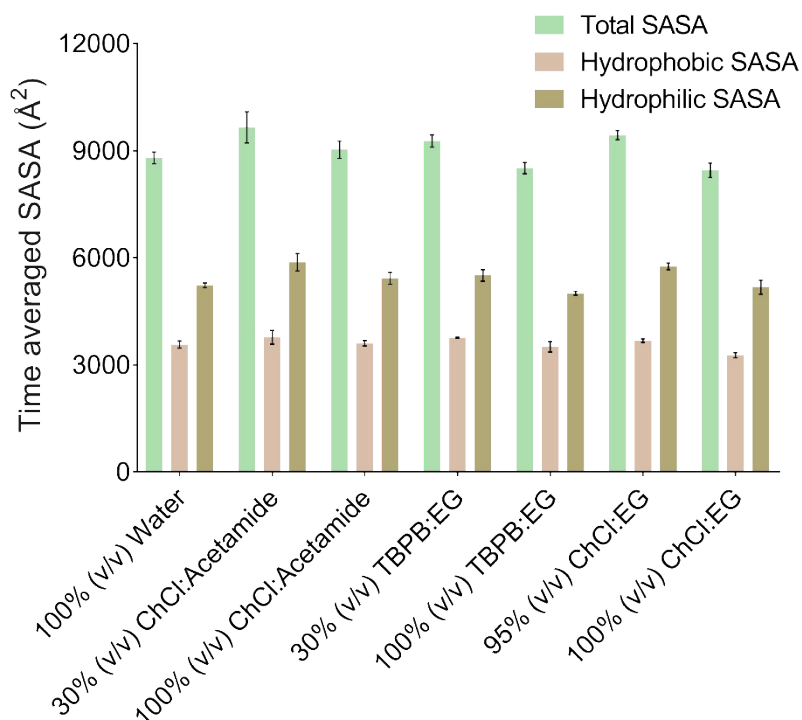


Figure S5. The time-averaged total solvent accessible surface area (SASA), hydrophobic SASA, and hydrophilic SASA of BSLA WT. All DES systems 30% (v/v) ChCl:Acetamide, 100% (v/v) ChCl:Acetamide, 30% (v/v) TBPB:EG, 100% (v/v) TBPB:EG, 95% (v/v) ChCl:EG and 100% (v/v) ChCl:EG have a molar ratio of 1:2. The data averaged from three independent runs. Error bars correspond to the standard deviation of three independent MD runs.

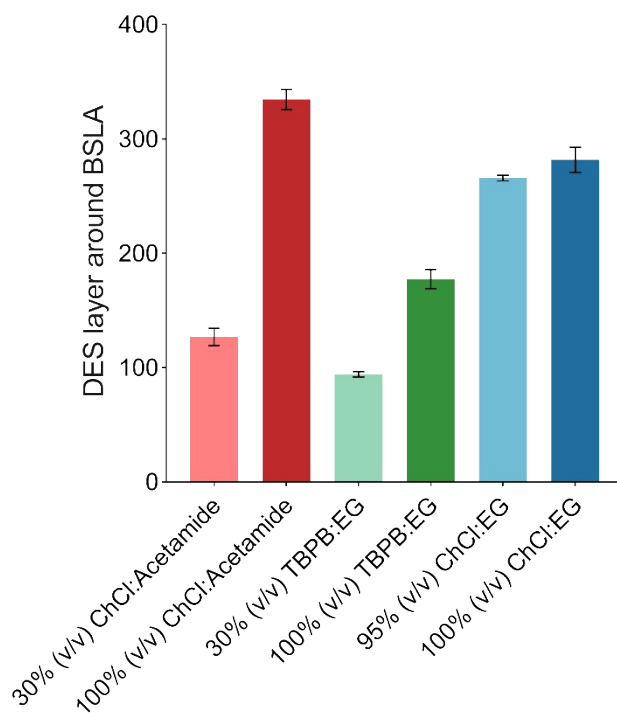


Figure S6. DES layer around BSLA. All DES systems 30% (v/v) ChCl:Acetamide, 100% (v/v) ChCl:Acetamide, 30% (v/v) TBPB:EG, 100% (v/v) TBPB:EG, 95% (v/v) ChCl:EG and 100% (v/v) ChCl:EG have a molar ratio of 1:2. The data averaged from three independent runs. Error bars correspond to the standard deviation of three independent MD runs.

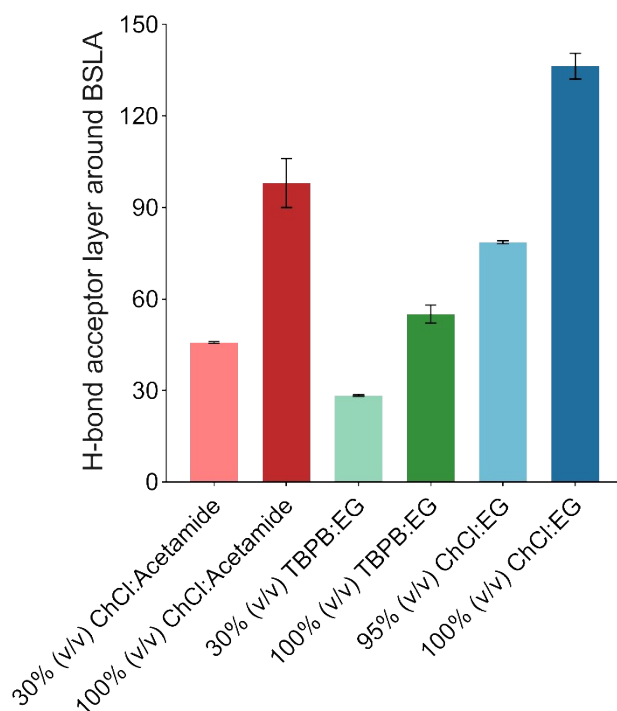


Figure S7. H-bond acceptor layer around BSLA. All DES systems 30% (v/v) ChCl:Acetamide, 100% (v/v) ChCl:Acetamide, 30% (v/v) TBPB:EG, 100% (v/v) TBPB:EG, 95% (v/v) ChCl:EG and 100% (v/v) ChCl:EG have a molar ratio of 1:2. The data averaged from three independent runs. Error bars correspond to the standard deviation of three independent MD runs.

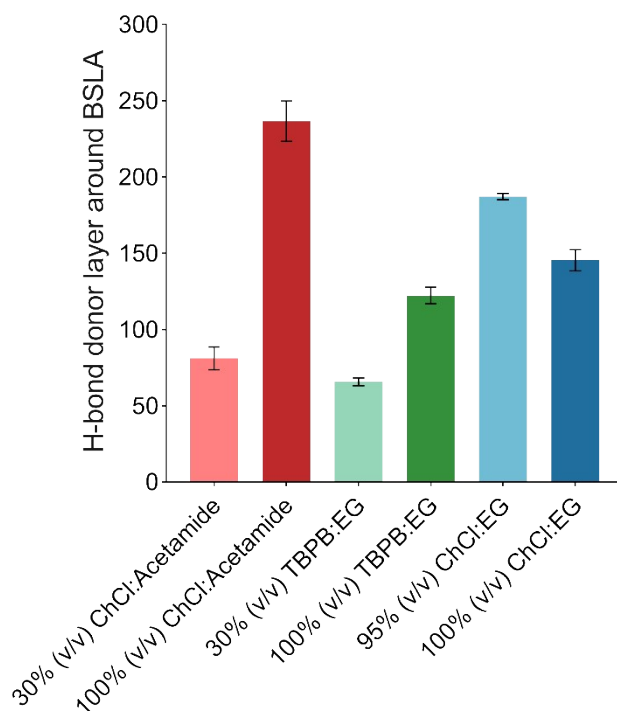


Figure S8. H-bond donor layer around BSLA. All DES systems 30% (v/v) ChCl:Acetamide, 100% (v/v) ChCl:Acetamide, 30% (v/v) TBPB:EG, 100% (v/v) TBPB:EG, 95% (v/v) ChCl:EG and 100% (v/v) ChCl:EG have a molar ratio of 1:2. The data averaged from three independent runs. Error bars correspond to the standard deviation of three independent MD runs.

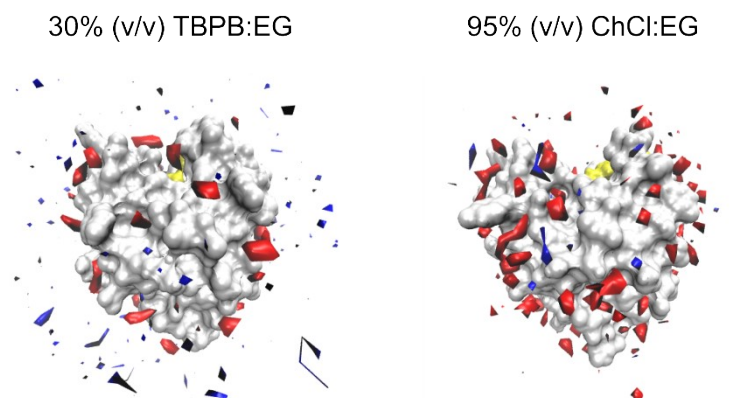


Figure S9. Spatial distribution of DES and water molecules at the enzyme surface in 30% (v/v) TBPB:EG, and 95% (v/v) ChCl:EG. The BSLA surface is shown in gray, the DES molecules are in red, and the water molecules are in blue. The active sites in BSLA (Ser 77, Asp 133, and His 156) are shown in yellow.

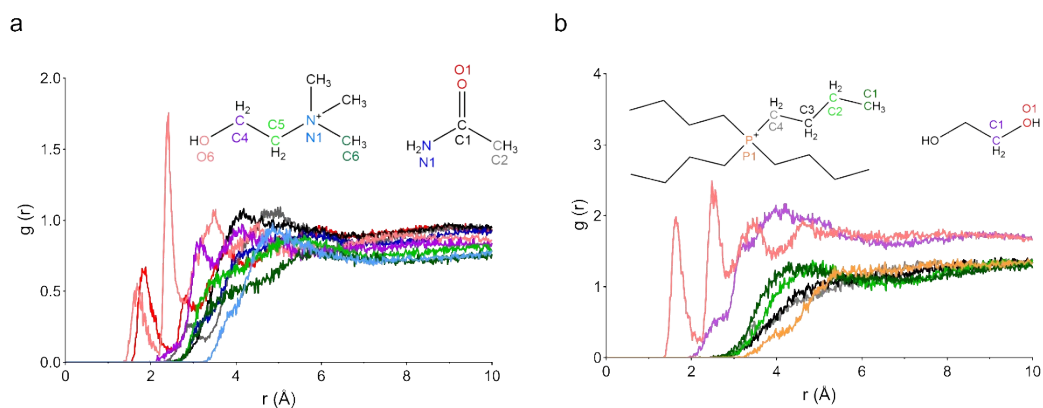


Figure S10. The RDFs were calculated in ChCl: acetamide and TBPB: EG systems. The choline⁺-N1, choline⁺-C4, choline⁺-C5, choline⁺-C6, choline⁺-O6, acetamide-N1, acetamide-O1, tetrabutylphosphonium⁺-P1, tetrabutylphosphonium⁺-C1, tetrabutylphosphonium⁺-P1, ethylene glycol-O1, and ethylene glycol-C1 around the BSLA residues, respectively.

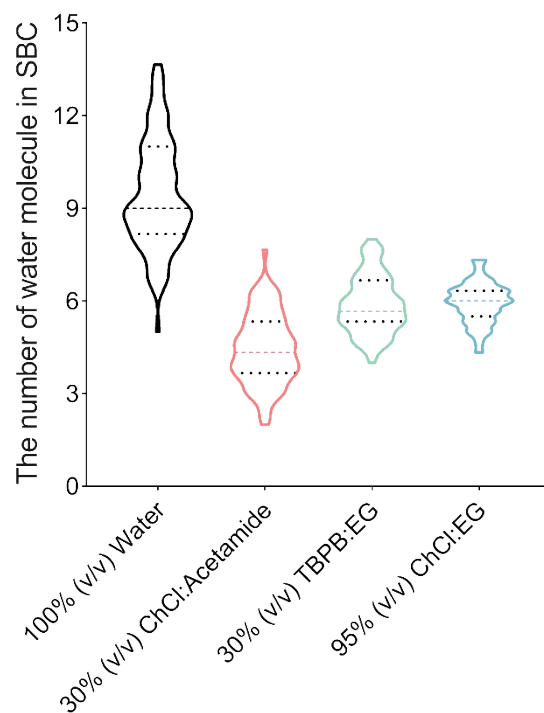


Figure S11. The water number in substrate binding cleft (SBC) of BSLA. All DES systems 30% (v/v) ChCl:Acetamide, 30% (v/v) TBPB:EG, and 95% (v/v) ChCl:EG have a molar ratio of 1:2. The data averaged from three independent runs.

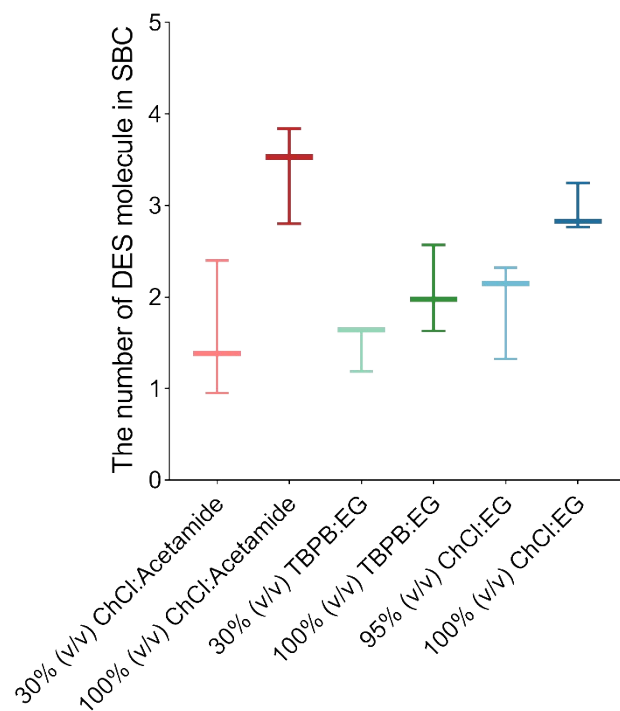


Figure S12. The number of DES molecule in substrate binding cleft (SBC) of BSLA. All DES systems 30% (v/v) ChCl:Acetamide, 100% (v/v) ChCl:Acetamide, 30% (v/v) TBPB:EG, 100% (v/v) TBPB:EG, 95% (v/v) ChCl:EG and 100% (v/v) ChCl:EG have a molar ratio of 1:2. The data averaged from three independent runs.

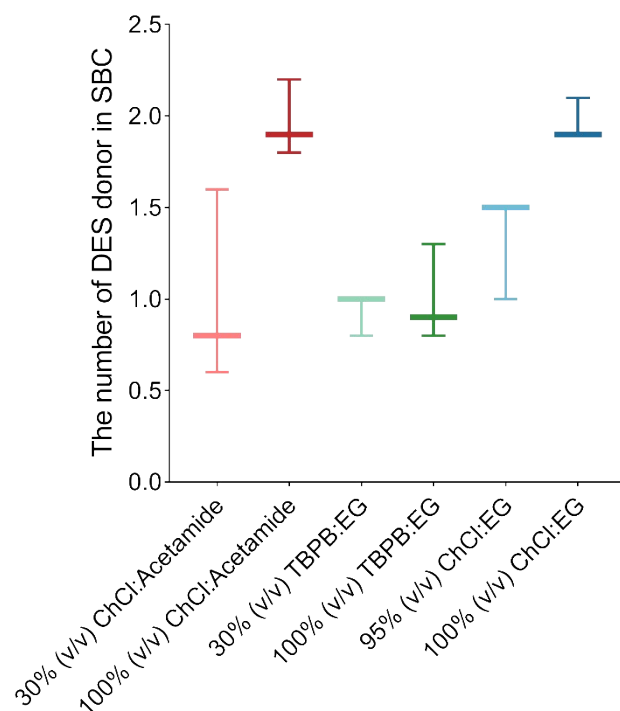


Figure S13. The number of DES donor in substrate binding cleft (SBC) of BSLA. All DES systems 30% (v/v) ChCl:Acetamide, 100% (v/v) ChCl:Acetamide, 30% (v/v) TBPB:EG, 100% (v/v) TBPB:EG, 95% (v/v) ChCl:EG and 100% (v/v) ChCl:EG have a molar ratio of 1:2. The data averaged from three independent runs.

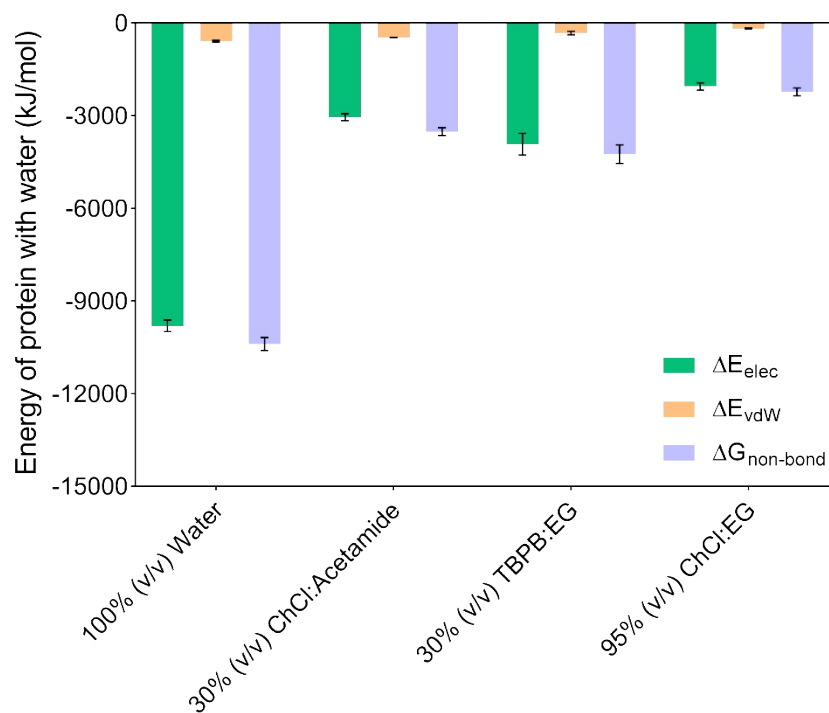


Figure S14. Time averaged energy of protein with water molecules. All DES systems 30% (v/v) ChCl:Acetamide, 30% (v/v) TBPB:EG, and 95% (v/v) ChCl:EG have a molar ratio of 1:2. The data averaged from three independent runs. The error bar was calculated from three independent MD runs. ΔE_{elec} : electrostatic energy. ΔE_{vdW} : van der Waals. $\Delta G_{nonbond}$: the non-bond binding. $\Delta G_{nonbond} = \Delta E_{elec} + \Delta E_{vdW}$.

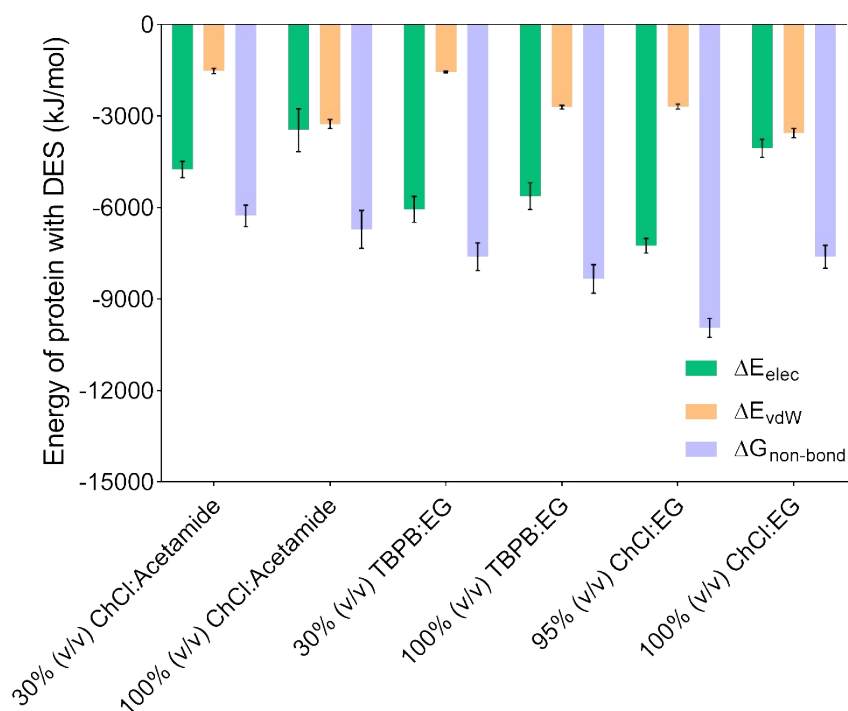


Figure S15. Time averaged energy of protein with DES molecules. All DES systems 30% (v/v) ChCl:Acetamide, 100% (v/v) ChCl:Acetamide, 30% (v/v) TBPB:EG, 100% (v/v) TBPB:EG, 95% (v/v) ChCl:EG and 100% (v/v) ChCl:EG have a molar ratio of 1:2. The data averaged from three independent runs. The error bar was calculated from three independent MD runs. ΔE_{elec} : electrostatic energy. ΔE_{vdW} : van der Waals energy. $\Delta G_{nonbond}$: the non-bond binding free energy. $\Delta G_{nonbond} = \Delta E_{elec} + \Delta E_{vdW}$.

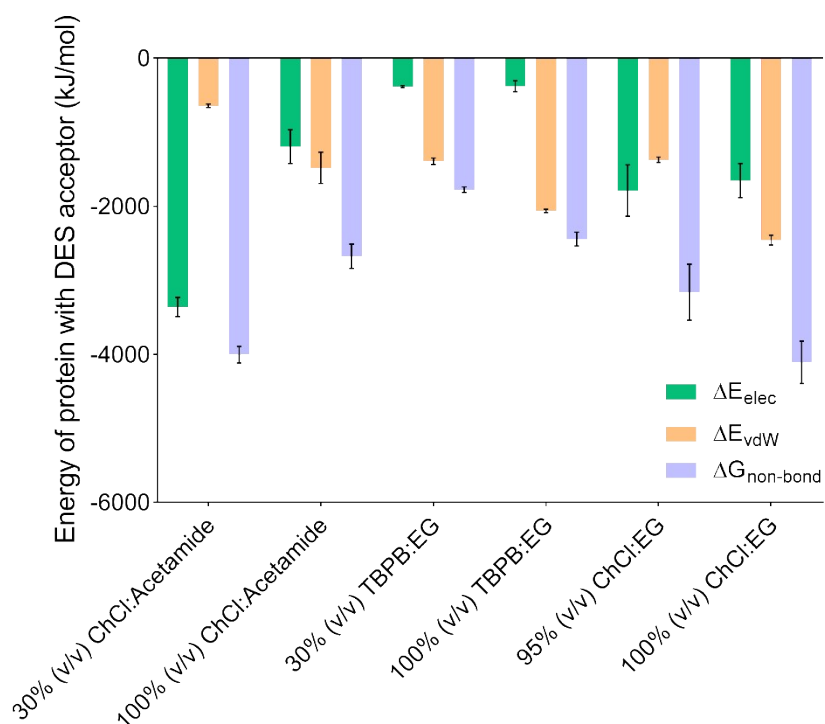


Figure S16. Time averaged energy of protein with DES acceptor. All DES systems 30% (v/v) ChCl:Acetamide, 100% (v/v) ChCl:Acetamide, 30% (v/v) TBPB:EG, 100% (v/v) TBPB:EG, 95% (v/v) ChCl:EG and 100% (v/v) ChCl:EG have a molar ratio of 1:2. The data averaged from three independent runs. The error bar was calculated from three independent MD runs. ΔE_{elec} : electrostatic energy. ΔE_{vdW} : van der Waals energy. $\Delta G_{nonbond}$: the non-bond binding free energy. $\Delta G_{nonbond} = \Delta E_{elec} + \Delta E_{vdW}$.

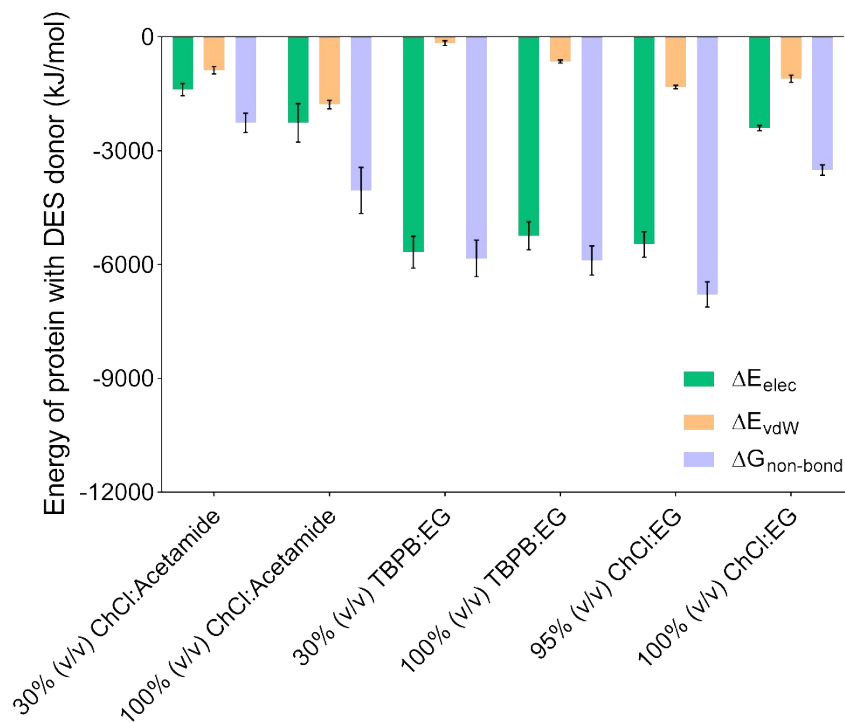


Figure S17. Time averaged energy of protein with DES donor. All DES systems 30% (v/v) ChCl:Acetamide, 100% (v/v) ChCl:Acetamide, 30% (v/v) TBPB:EG, 100% (v/v) TBPB:EG, 95% (v/v) ChCl:EG and 100% (v/v) ChCl:EG have a molar ratio of 1:2. The data averaged from three independent runs. The error bar was calculated from three independent MD runs. ΔE_{elec} : electrostatic energy. ΔE_{vdW} : van der Waals energy. $\Delta G_{\text{nonbond}}$: the non-bond binding free energy. $\Delta G_{\text{nonbond}} = \Delta E_{\text{elec}} + \Delta E_{\text{vdW}}$.

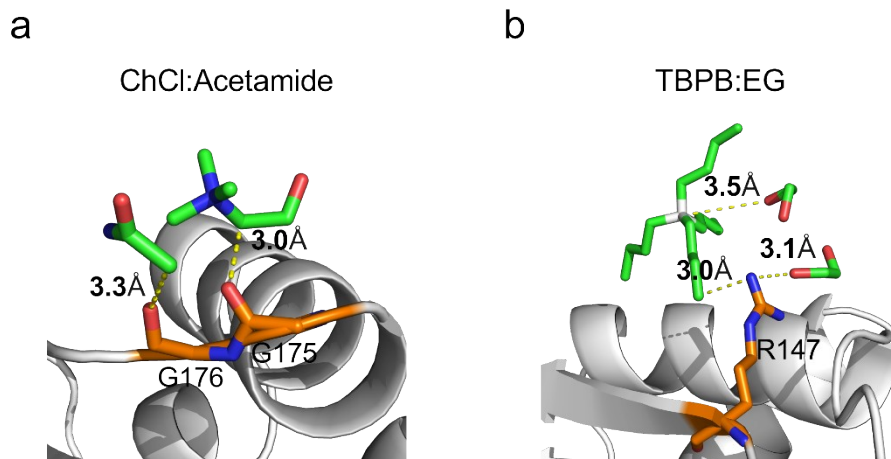


Figure S18. The interaction of residue (G175, G176, and R147) of BSLA with DES molecules (choline⁺, acetamide, tetrabutylphosphonium⁺, and ethylene glycol). In amino acids, orange represents C atoms, red represents O atoms, and blue represents N atoms, while in DES molecules, green represents C atoms, red represents O atoms, and white represents P atom. Hydrogen bonding forces are formed at distances less than 3.5 Å.

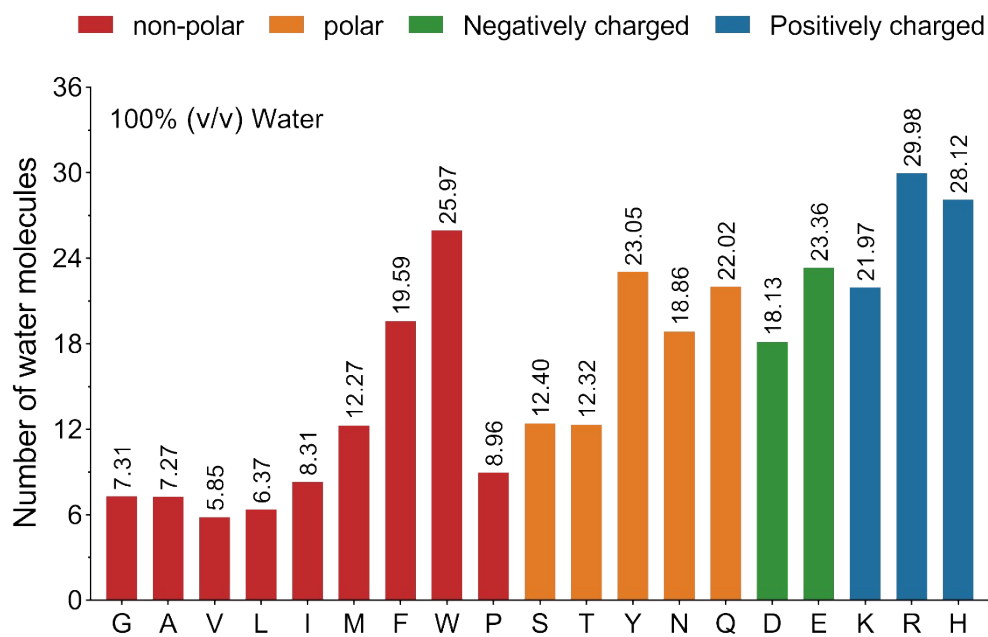


Figure S19. The number of water molecules around each amino acid type at the surface of BSLA WT in 100% water simulation system. The data were obtained from the average of three simulations. Red represents non-polar amino acids, orange represents polar amino acids, green represents negatively charged amino acids, and blue represents positively charged amino acids.

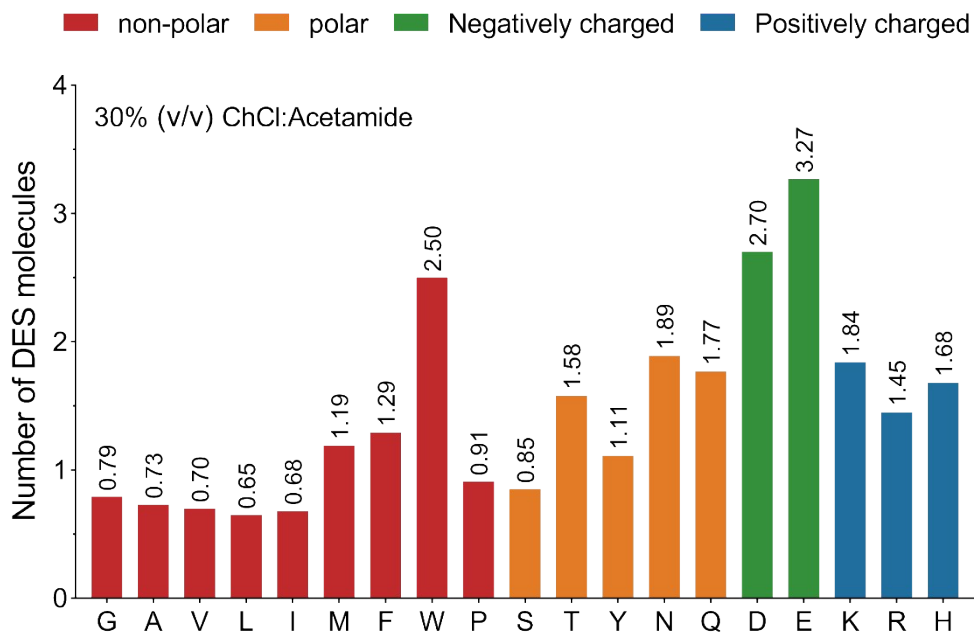


Figure S20. The number of DES molecules around each amino acid type at the surface of BSLA WT in 30% ChCl:Acetamide (1:2) simulation system. The data were obtained from the average of three simulations. Red represents non-polar amino acids, orange represents polar amino acids, green represents negatively charged amino acids, and blue represents positively charged amino acids.

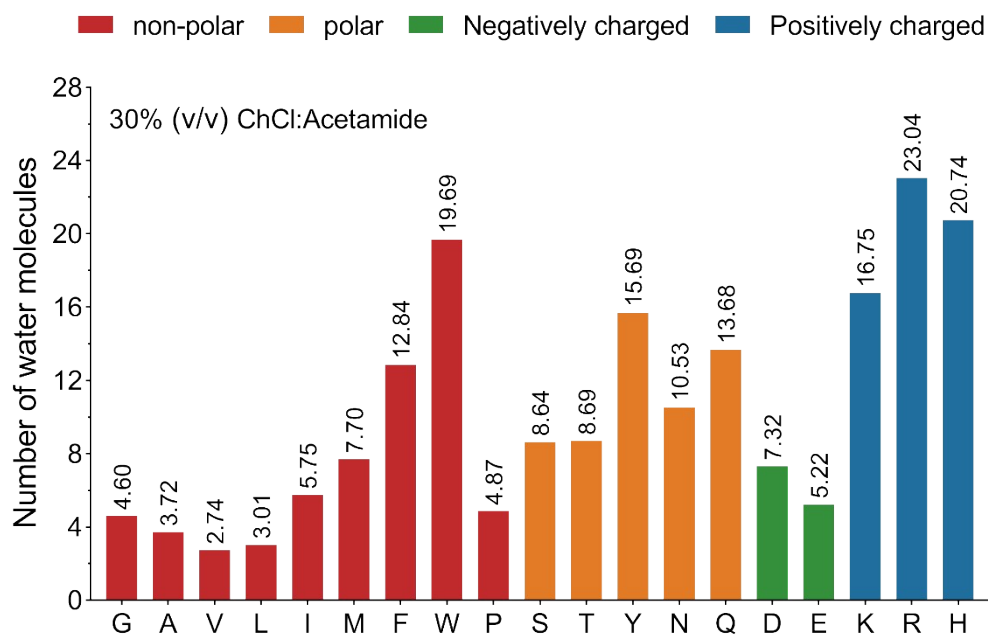


Figure S21. The number of water molecules around each amino acid type at the surface of BSLA WT in 30% ChCl:Acetamide (1:2) simulation system. The data were obtained from the average of three simulations. Red represents non-polar amino acids, orange represents polar amino acids, green represents negatively charged amino acids, and blue represents positively charged amino acids.

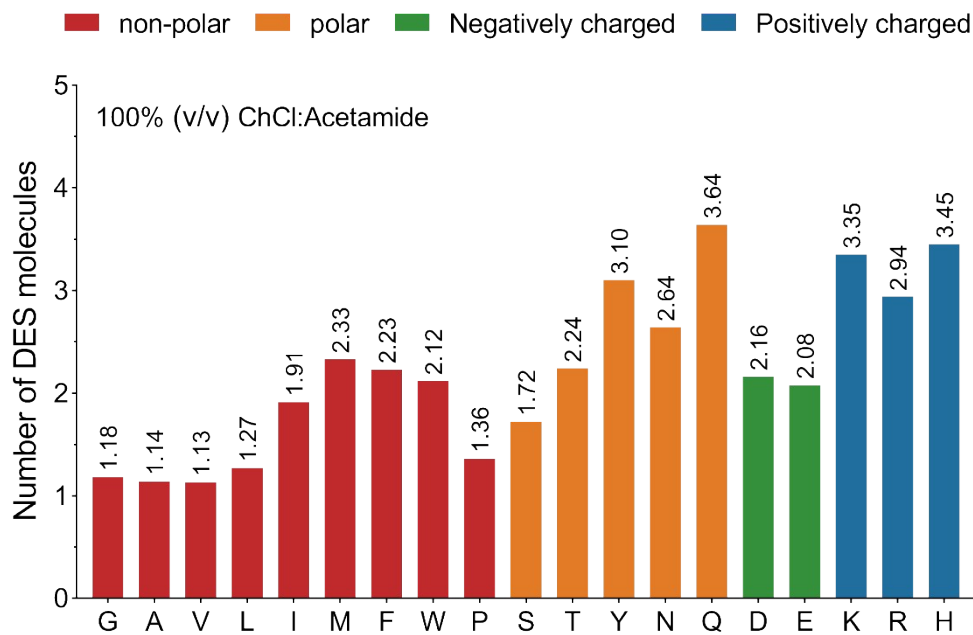


Figure S22. The number of DES molecules around each amino acid type at the surface of BSLA WT in 100% (v/v) ChCl:Acetamide (1:2) simulation system. The data were obtained from the average of three simulations. Red represents non-polar amino acids, orange represents polar amino acids, green represents negatively charged amino acids, and blue represents positively charged amino acids.

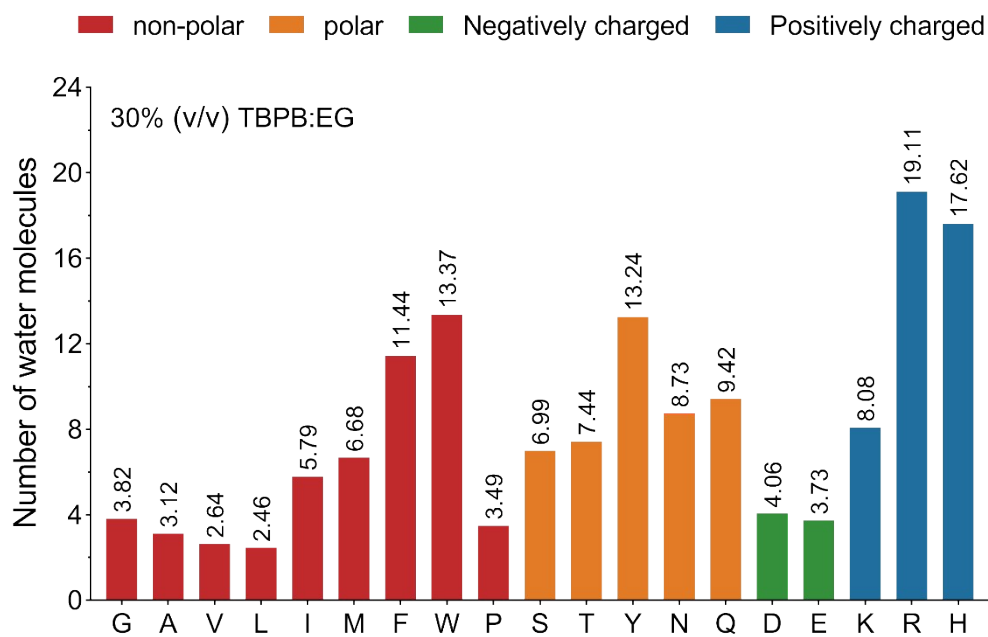


Figure S23. The number of water molecules around each amino acid type at the surface of BSLA WT in 30% (v/v) TBPB:EG (1:2) simulation system. The data were obtained from the average of three simulations. Red represents non-polar amino acids, orange represents polar amino acids, green represents negatively charged amino acids, and blue represents positively charged amino acids.

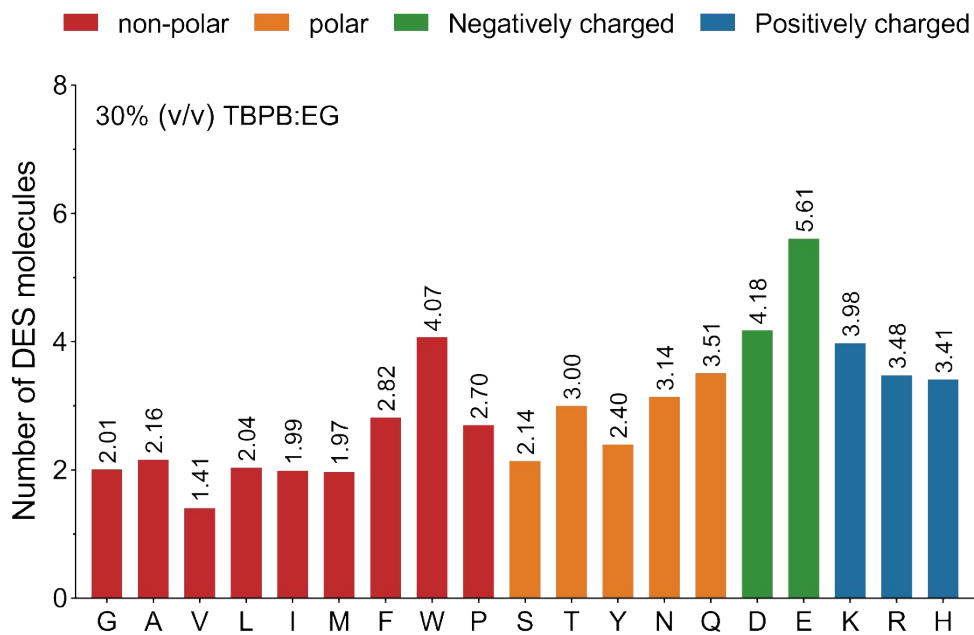


Figure S24. The number of DES molecules around each amino acid type at the surface of BSLA WT in 30% (v/v) TBPB:EG (1:2) simulation system. The data were obtained from the average of three simulations. Red represents non-polar amino acids, orange represents polar amino acids, green represents negatively charged amino acids, and blue represents positively charged amino acids.

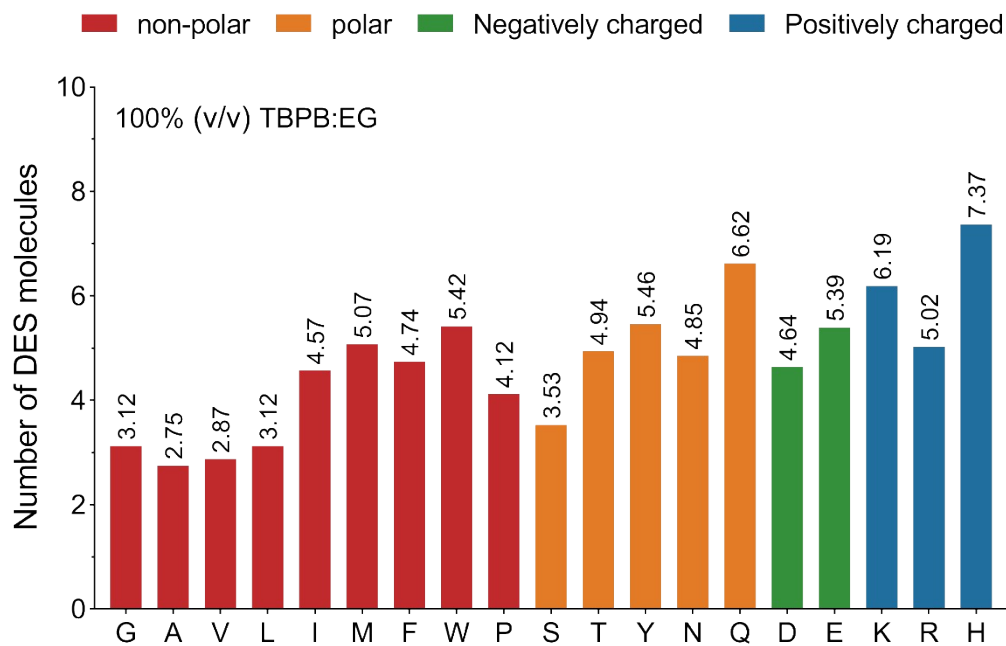


Figure S25. The number of DES molecules around each amino acid type at the surface of BSLA WT in 100% (v/v) TBPB:EG (1:2) simulation system. The data were obtained from the average of three simulations. Red represents non-polar amino acids, orange represents polar amino acids, green represents negatively charged amino acids, and blue represents positively charged amino acids.

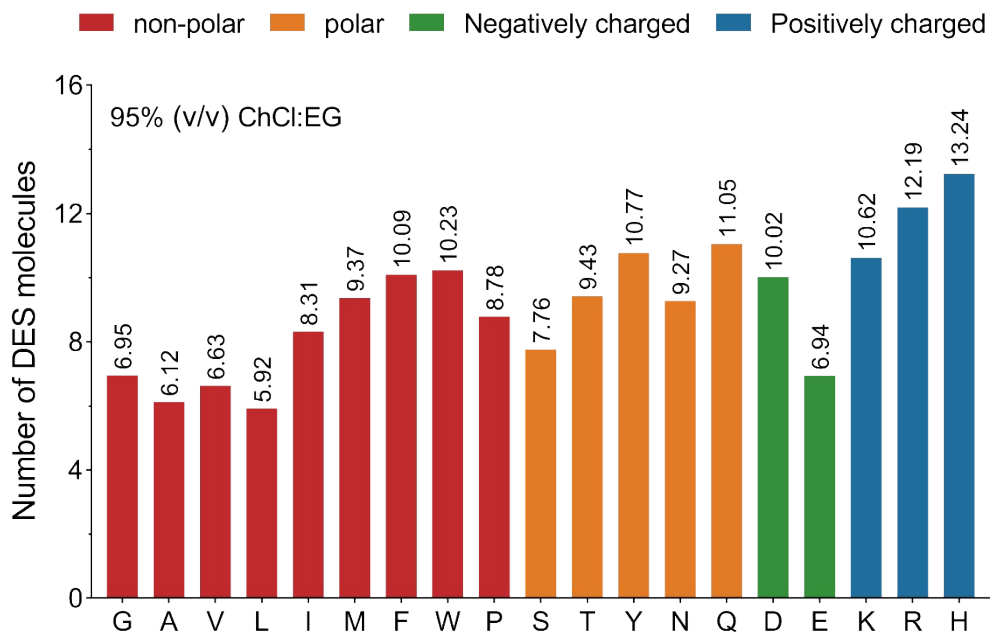


Figure S26. The number of DES molecules around each amino acid type at the surface of BSLA WT in 95% (v/v) ChCl:EG (1:2) simulation system. The data were obtained from the average of three simulations. Red represents non-polar amino acids, orange represents polar amino acids, green represents negatively charged amino acids, and blue represents positively charged amino acids.

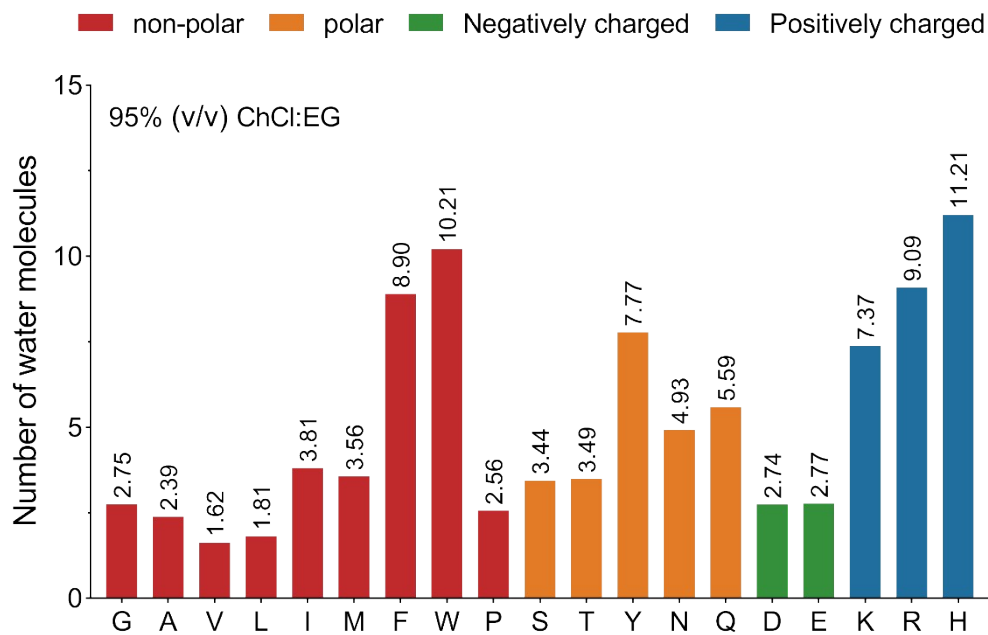


Figure S27. The number of water molecules around each amino acid type at the surface of BSLA WT in 95% (v/v) ChCl:EG (1:2) simulation system. The data were obtained from the average of three simulations. Red represents non-polar amino acids, orange represents polar amino acids, green represents negatively charged amino acids, and blue represents positively charged amino acids.

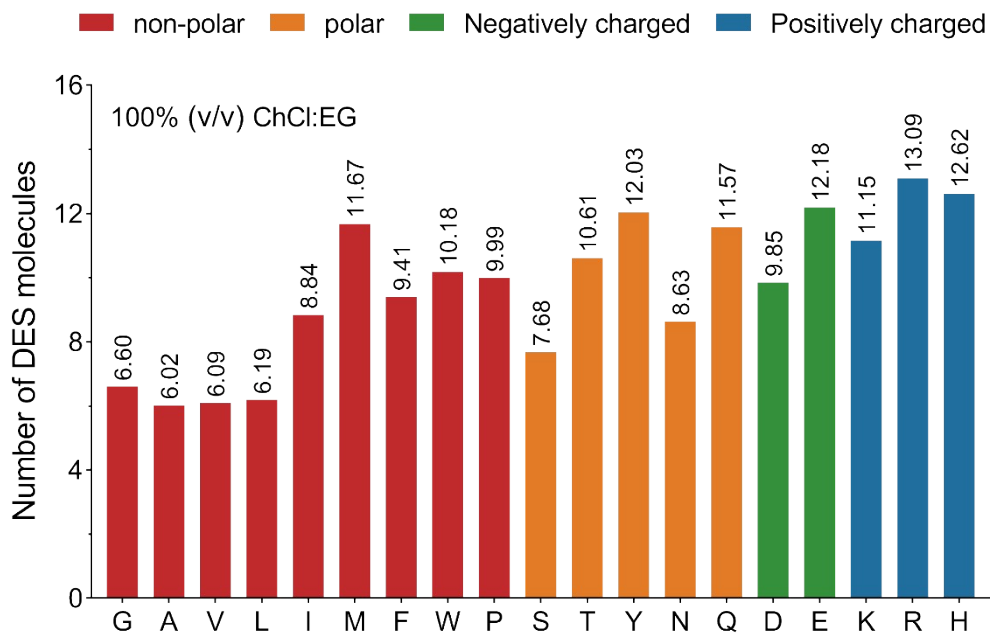


Figure S28. The number of DES molecules around each amino acid type at the surface of BSLA WT in 100% (v/v) ChCl:EG (1:2) simulation system. The data were obtained from the average of three simulations. Red represents non-polar amino acids, orange represents polar amino acids, green represents negatively charged amino acids, and blue represents positively charged amino acids.

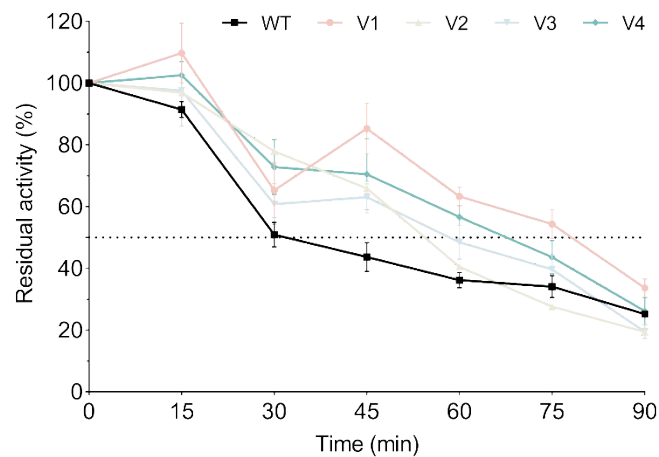


Figure S29. The residual activity of BSLA variants at 50°C as a function of time. Residual activity in buffer at the starting point was defined as 100%. The data were obtained from the average of at least three experiments. V1 (D64H/R142L), V2 (R107L/E171Y), V3 (D64H/R107L/E171Y), and V4 (D64H/R142L/E171Y).

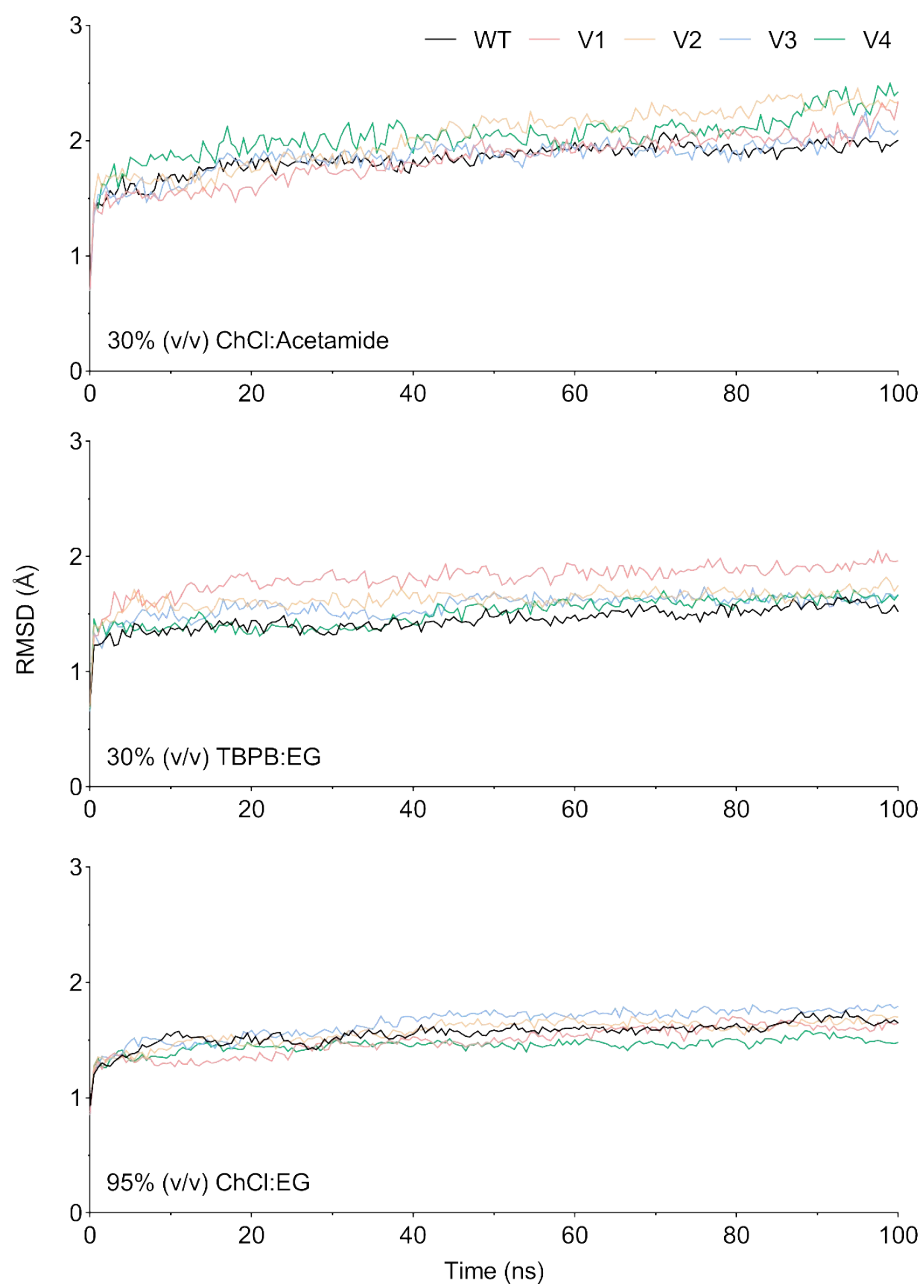


Figure S30. Root-mean-square deviation (RMSD) of the BSLA backbone with respect to the initial structure as a function of time in 30% (v/v) ChCl:Acetamide (1:2), 30% (v/v) TBPB:EG (1:2) and 95% (v/v) ChCl:EG (1:2). The RMSD value was average from three independent MD runs. V1 (D64H/R142L), V2 (R107L/E171Y), V3 (D64H/R107L/E171Y), and V4 (D64H/R142L/E171Y).

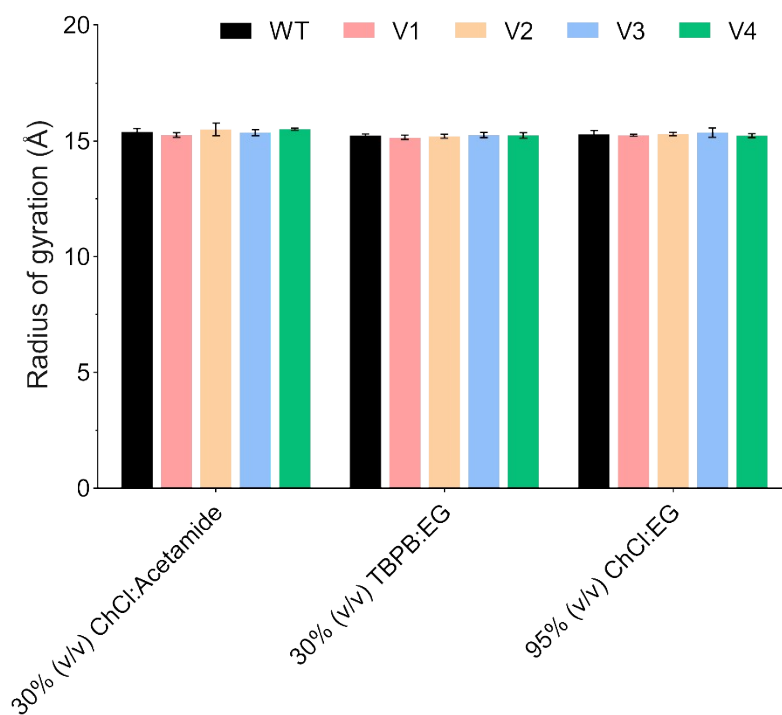


Figure S31. The time-averaged radius of gyration (R_g) of BSLA variants in 30% (v/v) ChCl:Acetamide (1:2), 30% (v/v) TBPB:EG (1:2) and 95% (v/v) ChCl:EG (1:2). The time-averaged R_g was calculated from the last 40 ns of the MD simulations. Error bars show the standard deviation from three independent MD runs. V1 (D64H/R142L), V2 (R107L/E171Y), V3 (D64H/R107L/E171Y), and V4 (D64H/R142L/E171Y).

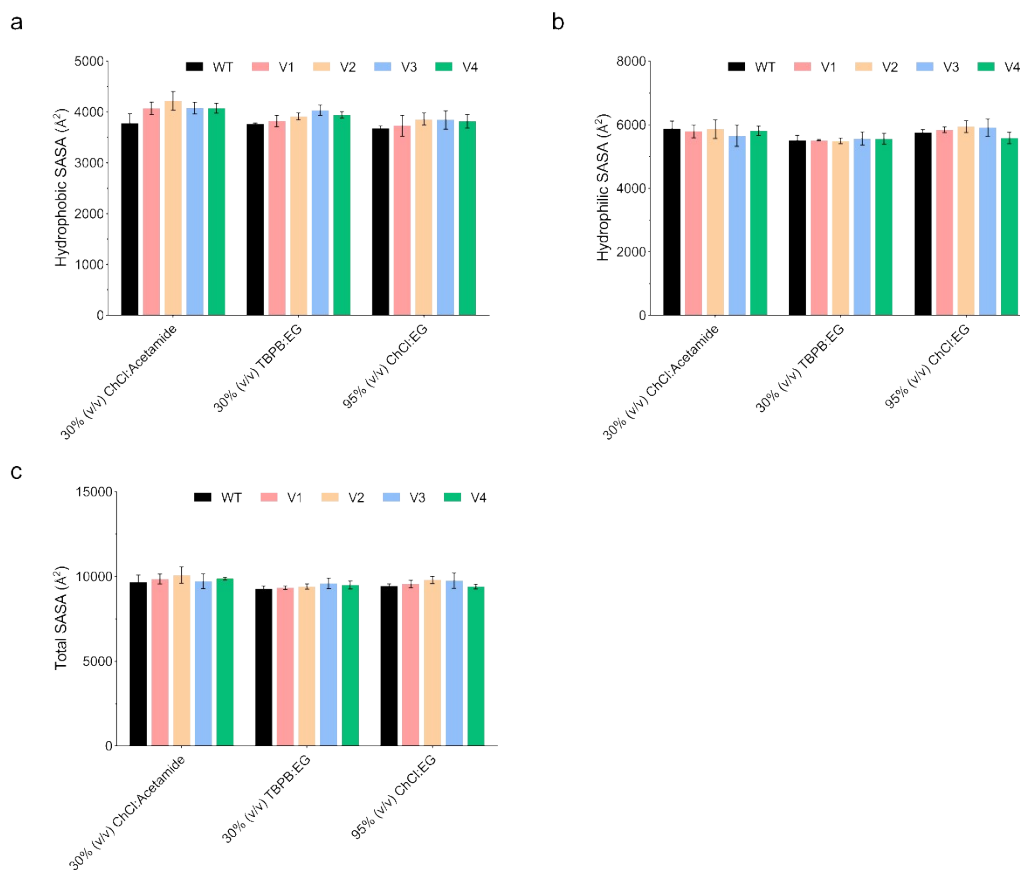


Figure S32. The time-averaged SASA of BSLA variants. (a) Hydrophobic SASA, (b) Hydrophilic SASA, and (c) Total SASA of BSLA variants in 30% (v/v) ChCl:Acetamide (1:2), 30% (v/v) TBPB:EG (1:2) and 95% (v/v) ChCl:EG (1:2). The time-averaged SASA was calculated from the last 40 ns of the MD simulations. Error bars show the standard deviation from three independent MD runs. V1 (D64H/R142L), V2 (R107L/E171Y), V3 (D64H/R107L/E171Y), and V4 (D64H/R142L/E171Y).

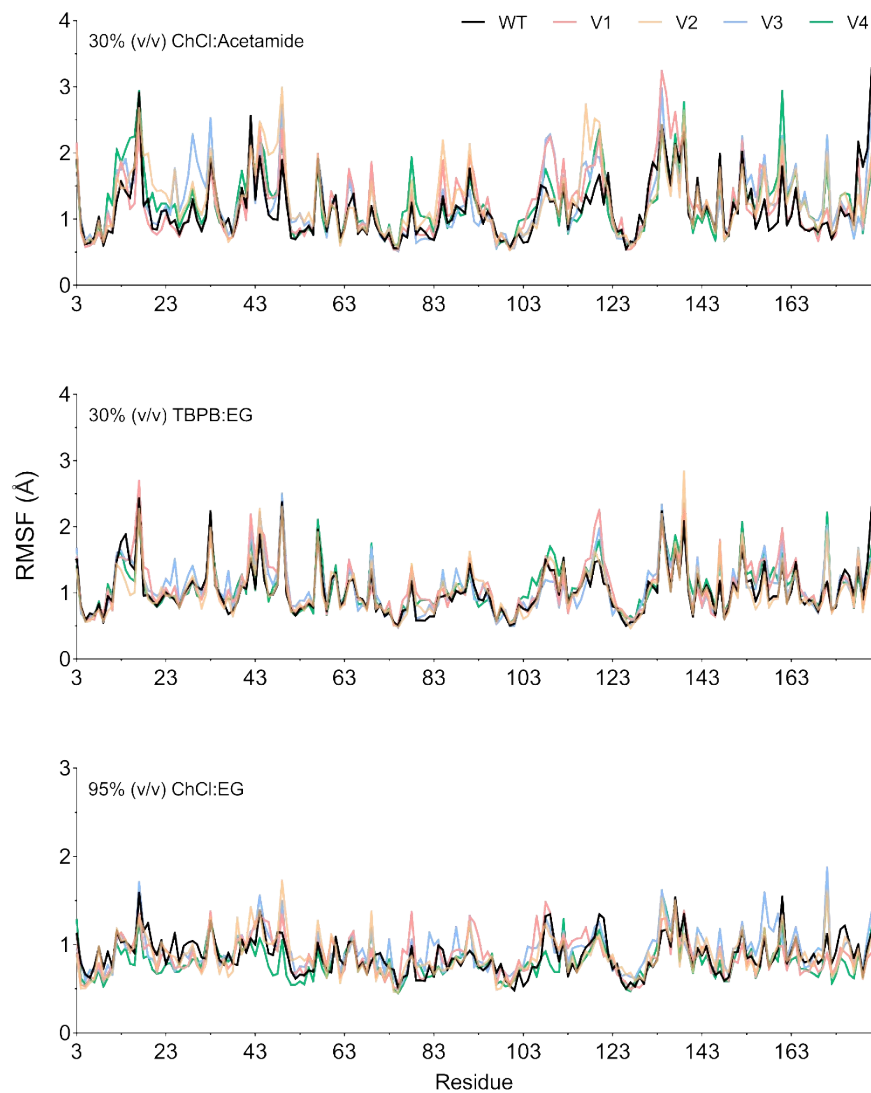


Figure S33. RMSF of BSLA variants in 30% (v/v) ChCl:Acetamide (1:2), 30% (v/v) TBPB:EG (1:2) and 95% (v/v) ChCl:EG (1:2) averaged over the last 40 ns of MD trajectories. The value average from three independent MD runs. V1 (D64H/R142L), V2 (R107L/E171Y), V3 (D64H/R107L/E171Y), and V4 (D64H/R142L/E171Y).

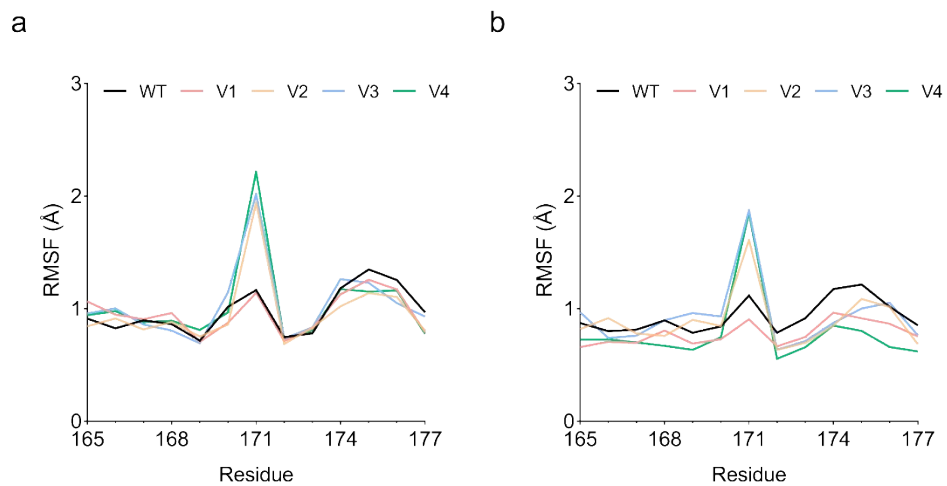


Figure S34. Local RMSF of BSLA variants in (a) 30% (v/v) TBPB:EG (1:2) and (b) 95% (v/v) ChCl:EG (1:2) averaged over the last 40 ns of MD trajectories. The value average from three independent MD runs. V1 (D64H/R142L), V2 (R107L/E171Y), V3 (D64H/R107L/E171Y), and V4 (D64H/R142L/E171Y).

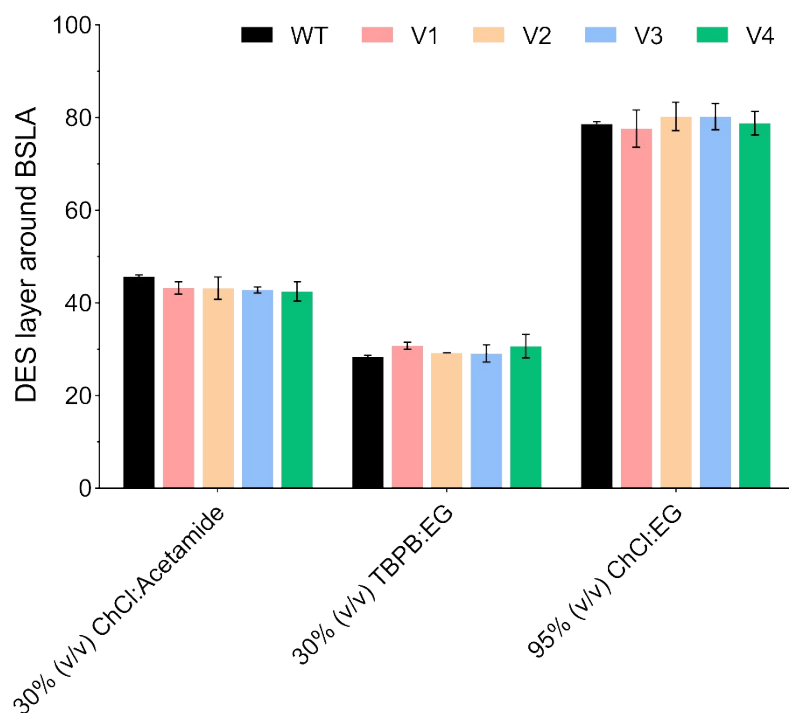


Figure S35. DES layer around BSLA variants in 30% (v/v) ChCl:Acetamide (1:2), 30% (v/v) TBPB:EG (1:2) and 95% (v/v) ChCl:EG (1:2) averaged over the last 40 ns of MD trajectories. Error bars show the standard deviation from three independent MD runs. V1 (D64H/R142L), V2 (R107L/E171Y), V3 (D64H/R107L/E171Y), and V4 (D64H/R142L/E171Y).

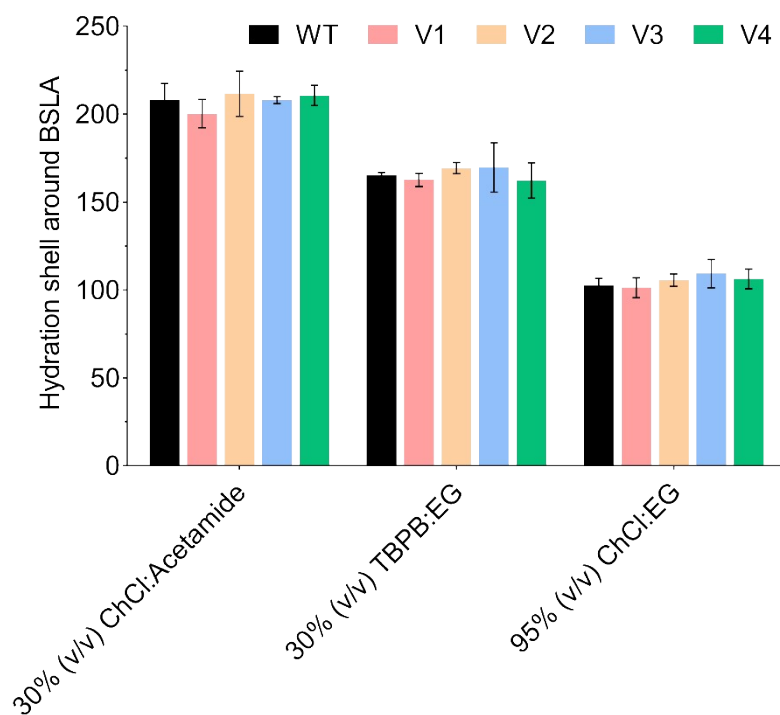


Figure S36. Hydration shell around BSLA variants in 30% (v/v) ChCl:Acetamide (1:2), 30% (v/v) TBPB:EG (1:2) and 95% (v/v) ChCl:EG (1:2) averaged over the last 40 ns of MD trajectories. Error bars show the standard deviation from three independent MD runs. V1 (D64H/R142L), V2 (R107L/E171Y), V3 (D64H/R107L/E171Y), and V4 (D64H/R142L/E171Y).

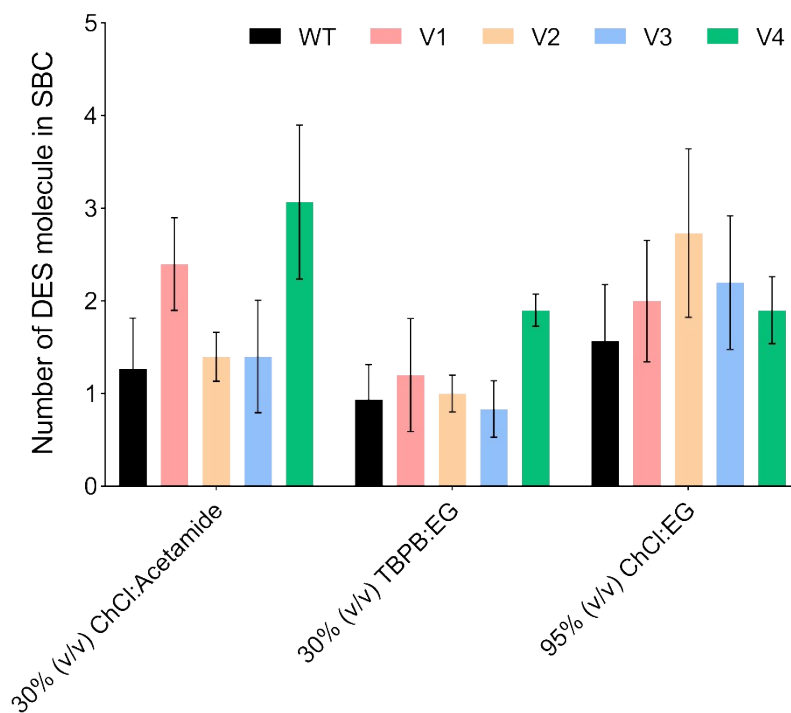


Figure S37. The number of DES molecule in substrate binding cleft (SBC) of BSLA variants in 30% (v/v) ChCl:Acetamide (1:2), 30% (v/v) TBPB:EG (1:2) and 95% (v/v) ChCl:EG (1:2) averaged over the last 40 ns of MD simulations. Error bars show the standard deviation from three independent MD runs. V1 (D64H/R142L), V2 (R107L/E171Y), V3 (D64H/R107L/E171Y), and V4 (D64H/R142L/E171Y).

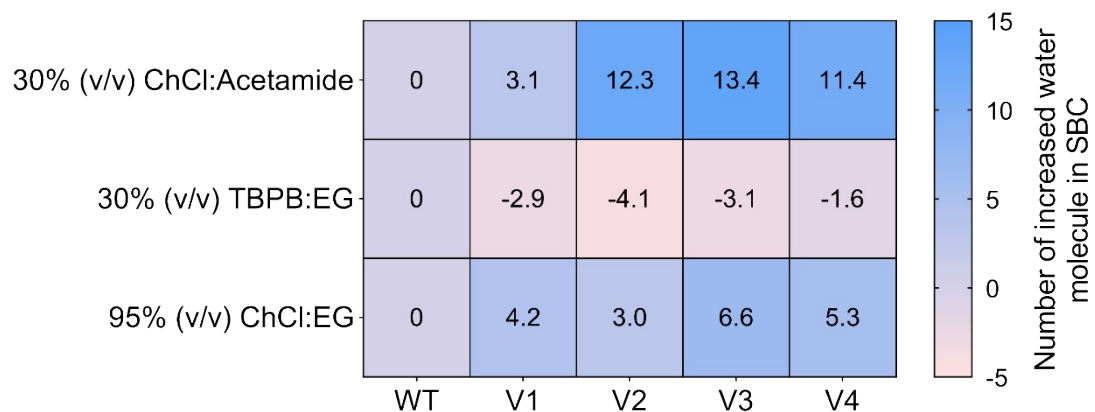


Figure S38. The number of increased water molecules in substrate binding cleft (SBC) of BSLA variants in 30% (v/v) ChCl:Acetamide (1:2), 30% (v/v) TBPB:EG (1:2) and 95% (v/v) ChCl:EG (1:2) averaged over the last 40 ns of MD simulations. The value average from three independent MD runs. V1 (D64H/R142L), V2 (R107L/E171Y), V3 (D64H/R107L/E171Y), and V4 (D64H/R142L/E171Y).

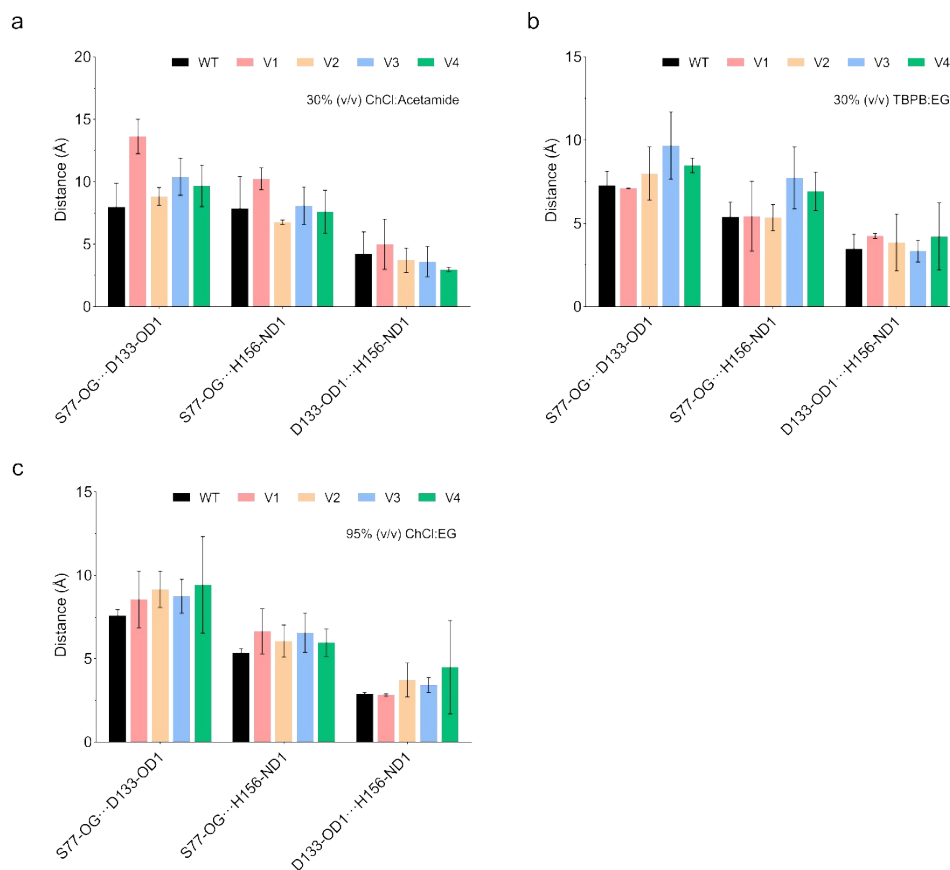


Figure S39. Distance of active site of BSLA variants. Distance (OG atom of Ser 77, OD1 atom of Asp 133, and ND1 atom of His 156) of BSLA variants in (a) 30% (v/v) ChCl:Acetamide (1:2), (b) (v/v) 30% TBPB:EG (1:2), and (c) 95% (v/v) ChCl:EG (1:2) averaged over the last 40 ns of MD simulations. Error bars show the standard deviation from three independent MD runs. V1 (D64H/R142L), V2 (R107L/E171Y), V3 (D64H/R107L/E171Y), and V4 (D64H/R142L/E171Y).

1. P. Liu, J.-W. Hao, L.-P. Mo and Z.-H. Zhang, *RSC Adv.*, 2015, **5**, 48675-48704.
2. H. Cui, L. Eltoukhy, L. Zhang, U. Markel, K.-E. Jaeger, M. D. Davari and U. Schwaneberg, *Angew. Chem. Int. Ed.*, 2021, **60**, 11448-11456.
3. M. Wang, Y. Sheng, H. Cui, A. Li, X. Li and H. Huang, *ACS Sustain. Chem. Eng.*, 2022, **10**, 15175-15185.
4. H. Cui, L. Zhang, L. Eltoukhy, Q. Jiang, S. K. Korkunc, K.-E. Jaeger, U. Schwaneberg and M. D. Davari, *ACS Catal.*, 2020, **10**, 14847-14856.
5. G. van Pouderoyen, T. Eggert, K. E. Jaeger and B. W. Dijkstra, *J. Mol. Biol.*, 2001, **309**, 215-226.
6. J. Qiao, Y. Sheng, M. Wang, A. Li, X. Li and H. Huang, *Angew. Chem. Int. Ed.*, 2023.
7. H. Cui, T. H. J. Stadtmueller, Q. Jiang, K.-E. Jaeger, U. Schwaneberg and M. D. Davari, *Chemcatchem*, 2020, **12**, 4073-4083.
8. X. Wang, Y. Sheng, H. Cui, J. Qiao, Y. Song, X. Li and H. Huang, *Angew. Chem. Int. Ed.*, 2023.
9. A. K. Malde, L. Zuo, M. Breeze, M. Stroet, D. Poger, P. C. Nair, C. Oostenbrink and A. E. Mark, *J. Chem. Theory Comput.*, 2011, **7**, 4026-4037.
10. P. Mark and L. Nilsson, *J. Phys. Chem. B*, 2001, **105**, 24A-24A.
11. H. Cui, L. Zhang, D. Soeder, X. Tang, M. D. Davari and U. Schwaneberg, *ACS Catal.*, 2021, **11**, 2445-2453.
12. X. Li, M. Wang, J. Qiao and H. Huang, *ACS Sustain. Chem. Eng.*, 2021, **9**, 14277-14287.
13. T. Makarewicz and R. Kazmierkiewicz, *J. Chem. Inf. Model.*, 2013, **53**, 1229-1234.
14. W. Humphrey, A. Dalke and K. Schulten, *J. mol. graph.*, 1996, **14**, 33-38, 27-38.
15. D. Van der Spoel, E. Lindahl, B. Hess, G. Groenhof, A. E. Mark and H. J. C. Berendsen, *J. Comput. Chem.*, 2005, **26**, 1701-1718.